

Exceptional Second-Order Topological Insulators

Yutaro Tanaka,^{1,*} Daichi Nakamura,^{2,†} Ryo Okugawa,^{3,‡} and Kohei Kawabata^{2,§}

¹*RIKEN Center for Emergent Matter Science, Wako, Saitama, 351-0198, Japan*

²*Institute for Solid State Physics, University of Tokyo, Kashiwa, Chiba 277-8581, Japan*

³*Department of Applied Physics, Tokyo University of Science, Tokyo 125-8585, Japan*

(Dated: November 12, 2024)

Point-gap topological phases of non-Hermitian systems exhibit exotic boundary states that have no counterparts in Hermitian systems. Here, we develop classification of second-order point-gap topological phases with reflection symmetry. Based on this classification, we propose exceptional second-order topological insulators, exhibiting second-order boundary states stabilized by point-gap topology. As an illustrative example, we uncover a two-dimensional exceptional second-order topological insulator with point-gapless corner states. Furthermore, we identify a three-dimensional exceptional second-order topological insulator that features hinge states with isolated exceptional points, representing second-order topological phases intrinsic to non-Hermitian systems. Our work enlarges the family of point-gap topological phases in non-Hermitian systems.

Introduction. Topological insulators have become a central concept in condensed matter physics [1, 2]. A characteristic feature of topological insulators is the bulk-boundary correspondence, where d -dimensional topological insulators possess $(d - 1)$ -dimensional boundary states characterized by bulk topological invariants. This framework extends to higher-order topological insulators: d -dimensional n th-order topological insulators support $(d - n)$ -dimensional boundary states [3–10].

Non-Hermiticity arises in effective descriptions of open classical and quantum systems [11–22], enriching topological phases and bulk-boundary correspondence [23, 24]. Complex energy spectra in non-Hermitian systems give rise to the concept of point gap [25–27]. A point gap is defined to be open when a region in the complex energy plane is devoid of the eigenstates with respect to a reference point. Topological phases characterized by a point gap are not necessarily continuously deformed to Hermitian phases and lead to exotic topological phenomena without Hermitian counterparts, such as non-Hermitian skin effects [26–61] and their higher-order [62–68] and defect-induced [69–71] extensions. These unique point-gap topological phases have been experimentally observed in various metamaterials [72–79], including two-dimensional (2D) systems [78–84].

Another notable feature of point-gap topological phases is the emergence of boundary states with anomalous complex energy dispersion [85–93], distinct from skin modes. These point-gap topological phases are called exceptional topological insulators [87]. Three-dimensional (3D) exceptional topological insulators exhibit surface states with the characteristic dispersion $k_x + ik_y$ or with an odd number of exceptional points (EPs). Thus, point-gap topology yields topological phases intrinsic to non-Hermitian systems. However, it has been largely unclear how non-Hermiticity diversifies higher-order topological phases and enriches boundary phenomena therein.

In this Letter, we develop classification of second-order point-gap topological phases with reflection sym-

metry. Based on this classification, we propose exceptional second-order topological insulators, non-Hermitian topological phases featuring point-gapless corner and hinge states. Our classification generally identifies possible second-order point-gap topology and uncovers previously unexplored second-order non-Hermitian topological phenomena. As a prototypical example, we introduce a 2D exceptional second-order topological insulator in class D that hosts corner states protected by pseudo-reflection symmetry. Furthermore, we present a 3D exceptional second-order topological insulator in class AIII + \mathcal{S}_- supporting point-gapless hinge states with a single EP, which has no counterparts in Hermitian second-order topological insulators. Our work expands the family of topological phases in non-Hermitian systems.

Classification of second-order point-gap topology. We classify reflection-symmetric second-order point-gap topology. We consider two types of reflection symmetry with respect to the mirror plane perpendicular to the i ($i = x, y, z$) direction:

$$\mathcal{M}H(k_i, \mathbf{k}_{\parallel})\mathcal{M}^{-1} = H(-k_i, \mathbf{k}_{\parallel}), \quad \mathcal{M}^2 = 1, \quad (1)$$

$$\tilde{\mathcal{M}}H^\dagger(k_i, \mathbf{k}_{\parallel})\tilde{\mathcal{M}}^{-1} = H(-k_i, \mathbf{k}_{\parallel}), \quad \tilde{\mathcal{M}}^2 = 1, \quad (2)$$

where \mathcal{M} and $\tilde{\mathcal{M}}$ are unitary matrices, and \mathbf{k}_{\parallel} denotes the wavevector except for the k_i component. We refer to Eq. (1) and Eq. (2) as reflection symmetry and pseudo-reflection symmetry, respectively. The latter is also called reflection symmetry[†] in the terminology of Ref. [27]. While these two types of reflection symmetry coincide with each other in Hermitian systems, this is not the case in non-Hermitian systems, leading to the rich topological classification.

Non-Hermitian Hamiltonians H are defined to have a point gap when their complex spectra do not cross a reference energy $E \in \mathbb{C}$ (i.e., $\det[H - E] \neq 0$) [26, 27]. To elucidate point-gap topology of H , we introduce a Her-

TABLE I. Classification of reflection-symmetric second-order point-gap topology in two and three dimensions. The non-trivial topological phases are shown with compatible reflection symmetry \mathcal{M} and pseudo-reflection symmetry $\tilde{\mathcal{M}}$ (or equivalently, reflection symmetry[†]). In the complex Altland-Zirnbauer class, the subscripts of \mathcal{S} specify the commutation (+) or anticommutation (−) relation with chiral symmetry, and the subscripts of \mathcal{M} and $\tilde{\mathcal{M}}$ specify the commutation (+) or anticommutation (−) relation with chiral and/or sublattice symmetry. In the real Altland-Zirnbauer^(†) class, the subscripts of \mathcal{M} and $\tilde{\mathcal{M}}$ specify the commutation (+) or anticommutation (−) relation with time-reversal and/or particle-hole symmetry^(†). The classification is extrinsic (i.e., termination-dependent) and allows for local breaking of reflection symmetry [94].

Class	$d = 2$	$d = 3$
A	$\mathbb{Z} (\mathcal{M})$	0
AIII	0	$\mathbb{Z} (\mathcal{M}_+, \tilde{\mathcal{M}}_-)$
AIII + \mathcal{S}_+	$\mathbb{Z} (\mathcal{M}_{\pm+}, \tilde{\mathcal{M}}_{\pm+})$	0
A + \mathcal{S}	$\mathbb{Z} \oplus \mathbb{Z} (\mathcal{M}_+)$	0
AIII + \mathcal{S}_-	0	$\mathbb{Z} \oplus \mathbb{Z} (\mathcal{M}_{++}, \tilde{\mathcal{M}}_{--})$
AI	$\mathbb{Z} (\mathcal{M}_+), 2\mathbb{Z} (\mathcal{M}_-)$	0
BDI	$\mathbb{Z}_2 (\mathcal{M}_{\pm\pm}, \tilde{\mathcal{M}}_{\pm\pm})$	$\mathbb{Z} (\mathcal{M}_{++}, \tilde{\mathcal{M}}_{-+}),$ $2\mathbb{Z} (\mathcal{M}_{--}, \tilde{\mathcal{M}}_{+-})$
D	$\mathbb{Z}_2 (\mathcal{M}_{\pm}, \tilde{\mathcal{M}}_+)$	$\mathbb{Z}_2 (\mathcal{M}_+, \tilde{\mathcal{M}}_+)$
DIII	0	$\mathbb{Z}_2 (\mathcal{M}_{++/-+/-},$ $\tilde{\mathcal{M}}_{++/-+/-})$
AII	$2\mathbb{Z} (\mathcal{M}_{\pm})$	0
CII	0	$2\mathbb{Z} (\mathcal{M}_{++/-}, \tilde{\mathcal{M}}_{+-/-})$
C	0	0
CI	0	0
AI [†]	0	0
BDI [†]	0	0
D [†]	$\mathbb{Z} (\mathcal{M}_+), 2\mathbb{Z} (\mathcal{M}_-)$	0
DIII [†]	$\mathbb{Z}_2 (\mathcal{M}_{\pm\pm}, \tilde{\mathcal{M}}_{\pm\pm})$	$\mathbb{Z} (\mathcal{M}_{++}, \tilde{\mathcal{M}}_{-+}),$ $2\mathbb{Z} (\mathcal{M}_{--}, \tilde{\mathcal{M}}_{+-})$
AII [†]	$\mathbb{Z}_2 (\mathcal{M}_{\pm}, \tilde{\mathcal{M}}_-)$	$\mathbb{Z}_2 (\mathcal{M}_+, \tilde{\mathcal{M}}_-)$
CII [†]	0	$\mathbb{Z}_2 (\mathcal{M}_{++/-+/-},$ $\tilde{\mathcal{M}}_{++/-+/-})$
C [†]	$2\mathbb{Z} (\mathcal{M}_{\pm})$	0
CI [†]	0	$2\mathbb{Z} (\mathcal{M}_{++/-}, \tilde{\mathcal{M}}_{+-/-})$

mitized Hamiltonians H defined by

$$H := \begin{pmatrix} 0 & H \\ H^\dagger & 0 \end{pmatrix}. \quad (3)$$

Point-gap topology of H coincides with Hermitian topology of H . We identify the relevant symmetry class of H for each internal symmetry class of H with additional reflection or pseudo-reflection symmetry (see Supplemental Material Sec. I [95]). We thus classify reflection-symmetric second-order point-gap topology in 2D and 3D non-Hermitian systems (Table I) from the classification

of Hermitian reflection-symmetric second-order topology [7, 94]. Table I specifies possible reflection-symmetric second-order point-gap topological phases and predicts previously unexplored second-order non-Hermitian topological phenomena, including both second-order skin effects [62, 63] and exceptional second-order topological insulators featuring point-gapless corner and hinge states. As illustrative examples, we below study a 2D exceptional second-order topological insulator in class D + $\tilde{\mathcal{M}}_+$ and a 3D exceptional second-order topological insulator in class AIII + $\mathcal{S}_- + \mathcal{M}_{++}$.

2D exceptional second-order topological insulator. We discuss exceptional second-order topological insulators in class D, where non-Hermitian Hamiltonians respect particle-hole symmetry

$$CH^T(\mathbf{k})C^{-1} = -H(-\mathbf{k}), \quad CC^* = 1, \quad (4)$$

with a unitary matrix C . The second-order point-gap topological phases are \mathbb{Z}_2 classified in the presence of pseudo-reflection ($\tilde{\mathcal{M}}_+$) symmetry in Eq. (2) commuting with C .

To capture boundary states of the exceptional second-order topological insulator, we analyze their low-energy continuum Hamiltonian in the presence of pseudo-reflection symmetry with respect to the y - z plane. We begin with a chiral edge state k_x of a 2D first-order point-gap topological phase in class D, which is \mathbb{Z}_2 classified [27]. To realize a second-order point-gap topological phase, we double this \mathbb{Z}_2 boundary state to trivialize the first-order topology. In the simultaneous presence of particle-hole with $C = \sigma_0$ and pseudo-reflection symmetries with $\tilde{\mathcal{M}}_+ = \sigma_x$, a generic non-Hermitian doubled boundary state is given as

$$H(k_x) = k_x \sigma_z + i\delta \sigma_y, \quad (\delta \in \mathbb{R}), \quad (5)$$

where σ_0 is the 2×2 identity matrix, and σ_i ($i = x, y, z$) are the Pauli matrices. The energy dispersion is $E(k_x) = \pm \sqrt{k_x^2 - \delta^2}$, showing the stability of the gapless points $k_x = \pm \delta$. Conversely, in the absence of pseudo-reflection symmetry, a particle-hole-symmetric perturbation $\delta' \sigma_y$ ($\delta' \in \mathbb{R}$) induces a point gap. Consequently, the boundary states remain gapless only in the presence of pseudo-reflection symmetry, implying the emergence of point-gapless states around pseudo-reflection-invariant corners.

We introduce a tight-binding model on a square lattice to realize a 2D exceptional second-order topological insulator

$$H_{\tilde{\mathcal{M}}}(\mathbf{k}) = \sin k_x \tau_x \sigma_z + (1 - \cos k_x - \cos k_y) \tau_y \\ + i \sin k_y \sigma_z + im_1 \tau_x \sigma_y + m_2 \tau_y \sigma_x, \quad (6)$$

where τ_i ($i = x, y, z$) are the Pauli matrices. This model respects particle-hole symmetry with $C = \sigma_0$ and pseudo-reflection symmetry with $\tilde{\mathcal{M}}_+ = \sigma_x$. The energy spectra of this Hamiltonian under the full periodic boundary

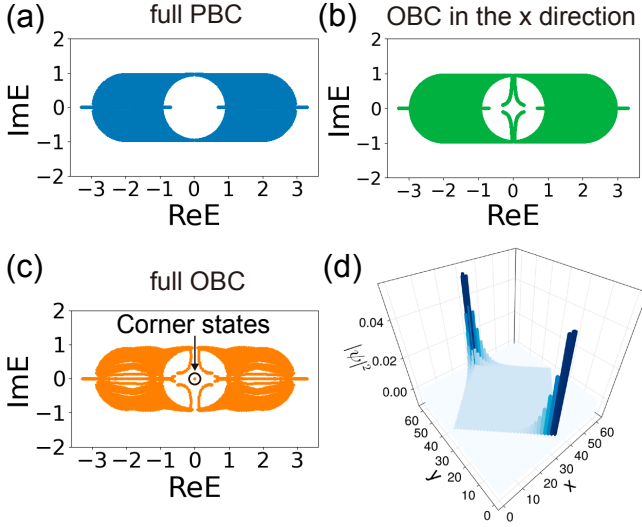


FIG. 1. (a-c) Complex energy spectra of the Hamiltonian (6) under the (a) full periodic boundary conditions (PBC), (b) open boundary conditions (OBC) in the x direction and PBC in the y direction, and (c) full OBC for a square crystal with the edges perpendicular to the $(1, 1)$ and $(1, -1)$ directions. (d) Real-space distribution of one of the right eigenstates encircled by the circle in (c). The parameters are $m_1 = 0.1$ and $m_2 = 0.3$. The system size is 51 in the x direction with the momentum resolution $\Delta k_y = 2\pi/10000$ in (b). The system size is 61 in the x and y directions in (c) and (d).

conditions (PBC) host a point gap at $E = 0$ [Fig. 1(a)]. Under the open boundary conditions (OBC) in the x direction, the point gap at $E = 0$ does not close [Fig. 1(b)] since the edges along the y direction are not invariant under the reflection $x \rightarrow -x$. On the other hand, the corner between the edges perpendicular to the $(1, 1)$ and $(1, -1)$ directions remains invariant under the reflection. Figures 1(c) and 1(d) illustrate the spectra under this boundary conditions, demonstrating the point-gap closing at $E = 0$ with the emergence of corner states. These corner states are protected by pseudo-reflection symmetry and localized at the reflection-invariant positions. We also show that the above second-order point-gap topological phases can be continuously deformed to a Hermitian topological phase (or more generally, line-gap topological phase) while keeping the point gap and symmetry (see Supplemental Material Sec. II [95]).

Layer construction of 3D exceptional second-order topological insulator. We construct 3D point-gap topological phases from 2D ones, which we refer to as layer construction. The layer construction is used for 3D Hermitian topological phases protected by spatial symmetry [96–101]. In the following, we generalize this method to non-Hermitian systems and construct a 3D exceptional second-order topological insulator protected by reflection symmetry.

We begin with the following tight-binding model of

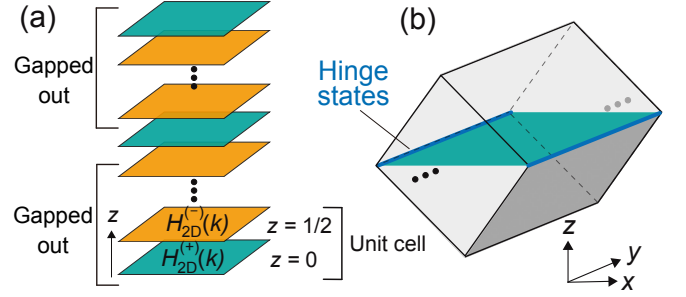


FIG. 2. (a) Layer construction for realizing a three-dimensional (3D) exceptional second-order topological insulator with reflection symmetry. The colors of the layers indicate the sign (\pm) of $H_{2D}^{(\pm)}(\mathbf{k})$. The dotted box indicates the unit cell. (b) 3D reflection-symmetric exceptional second-order topological insulator with hinge states by the layer construction.

a 2D exceptional topological insulator as layers to be stacked:

$$H_{2D}^{(\pm)}(\mathbf{k}) = \begin{pmatrix} 0 & h_1^{(\pm)}(\mathbf{k}) \\ h_2^{(\pm)}(\mathbf{k}) & 0 \end{pmatrix}, \quad (7)$$

with the off-diagonal parts $h_1^{(\pm)}(\mathbf{k})$ and $h_2^{(\pm)}(\mathbf{k})$

$$\begin{aligned} h_1^{(\pm)}(\mathbf{k}) &= \pm[(1 - \cos k_x - \cos k_y)\sigma_x + \sin k_x \sigma_y \\ &\quad + i \sin k_y \sigma_0], \\ h_2^{(\pm)}(\mathbf{k}) &= \pm[(-3 - \cos k_x - \cos k_y)\sigma_x + \sin k_x \sigma_y \\ &\quad + i \sin k_y \sigma_0 + i \Delta \sigma_z]. \end{aligned} \quad (8)$$

Below, we choose $\Delta = 0.01$. Both $H_{2D}^{(+)}(\mathbf{k})$ and $H_{2D}^{(-)}(\mathbf{k})$ respect chiral and sublattice symmetries,

$$\Gamma H^\dagger(\mathbf{k}) \Gamma^{-1} = -H(\mathbf{k}), \quad (9)$$

$$\mathcal{S} H(\mathbf{k}) \mathcal{S}^{-1} = -H(\mathbf{k}), \quad (10)$$

with $\Gamma = \tau_x \sigma_z$ and $\mathcal{S} = \tau_z \sigma_0$. Hence, they belong to class AIII + \mathcal{S}_- and exhibit 2D point-gap topology and concomitant boundary states with a single EP (see Supplemental Material Sec. III [95]) [88, 92]. This topological phase is characterized by a pair of the Chern numbers of the two Hermitian matrices $ih_1^{(\pm)}\sigma_z$ and $ih_2^{(\pm)}\sigma_z$: $(\text{Ch}_1, \text{Ch}_2) := (\text{Ch}[ih_1^{(\pm)}\sigma_z], \text{Ch}[ih_2^{(\pm)}\sigma_z])$ [27]. These Chern numbers for $H_{2D}^{(+)}(\mathbf{k})$ and $H_{2D}^{(-)}(\mathbf{k})$ are given by $(\text{Ch}_1, \text{Ch}_2) = (+1, 0)$ and $(\text{Ch}_1, \text{Ch}_2) = (-1, 0)$, respectively.

We alternately stack $H_{2D}^{(+)}(\mathbf{k})$ and $H_{2D}^{(-)}(\mathbf{k})$ layers along the z direction, as shown in Fig. 2(a). Each unit cell contains one $H_{2D}^{(+)}(\mathbf{k})$ layer and one $H_{2D}^{(-)}(\mathbf{k})$, positioned at $z = n$ and $z = n + 1/2$, respectively, where n is a nonnegative integer, and the size of the unit cell in the z direction is 1. By introducing the interlayer coupling

$H_z(\mathbf{k})$, the Bloch Hamiltonian of the stacked layers is given by

$$H_{\mathcal{M}}(\mathbf{k}) = \begin{pmatrix} H_{2D}^{(+)}(\mathbf{k}) & H_z(\mathbf{k}) \\ H_z^\dagger(\mathbf{k}) & H_{2D}^{(-)}(\mathbf{k}) \end{pmatrix}, \quad (11)$$

where $H_z(\mathbf{k})$ is a 4×4 matrix expressed as

$$H_z(\mathbf{k}) = (1 + e^{-ik_z})(t_1\tau_x\sigma_x + it_2\tau_y\sigma_z). \quad (12)$$

The Pauli matrices τ_i and σ_i correspond to the degrees of freedom in each layer. Henceforth, we assume that the number of layers is odd so that reflection symmetry with respect to the x - y plane will be satisfied.

This construction leads to a reflection-symmetric exceptional second-order topological insulator with point-gapless hinge states. As shown in Fig. 2(a), while pairs of the layers are trivialized due to their Chern numbers of different signs, a single layer at the reflection center maintains topological edge states, resulting in the one-dimensional hinge states [Fig. 2(b)]. Inheriting from the edge states of the original 2D exceptional topological insulators [i.e., Eq. (7)], the hinge state also possesses a single EP. This discussion extends the layer construction of second-order topological insulators from Chern insulators [102–106] to exceptional second-order topological insulators. While we have focused on reflection symmetry, we also show that inversion symmetry leads to a 3D exceptional second-order topological insulator in Supplemental Material Sec. IV [95].

The Hamiltonian $H_{\mathcal{M}}(\mathbf{k})$ respects reflection symmetry in Eq. (1) with respect to the x - y plane. Here, the symmetry representation is given by $\mathcal{M} = \text{diag}(1, e^{-ik_z})$, which acts on the sublattice degrees of freedom $z = 0$ and $z = 1/2$. The model $H_{\mathcal{M}}(\mathbf{k})$ also respects chiral symmetry in Eq. (9) and sublattice symmetry in Eq. (10). Therefore, $H_{\mathcal{M}}(\mathbf{k})$ belongs to class AIII + \mathcal{S}_- in the 38-fold symmetry classes [27]. Since both Γ and \mathcal{S} commute with \mathcal{M} , the second-order point-gap topology in $H_{\mathcal{M}}(\mathbf{k})$ is classified as $\mathbb{Z} \oplus \mathbb{Z}$ (see class AIII + \mathcal{S}_- with \mathcal{M}_{++} in Table I).

Topology of 3D exceptional second-order topological insulator. We show that a 3D exceptional second-order topological insulator indeed emerges in the Hamiltonian in Eq. (11). On the reflection-invariant plane $k_z = k_0$ ($= 0, \pi$), the Hamiltonian $H_{\mathcal{M}}(k_x, k_y, k_0)$ is block diagonalizable: $H_+(k_x, k_y, k_0) \oplus H_-(k_x, k_y, k_0)$, where $H_+(k_x, k_y, k_0)$ and $H_-(k_x, k_y, k_0)$ are the matrices labeled by the reflection-symmetry eigenvalues ± 1 , respectively. Since \mathcal{M} commutes with both chiral and sublattice symmetries, each sector belongs to class AIII + \mathcal{S}_- . Owing to the preservation of sublattice symmetry, $H_{\pm}(k_x, k_y, k_0)$ is given by

$$H_{\pm}(k_x, k_y, k_0) = \begin{pmatrix} 0 & h_{1,\pm}(k_x, k_y, k_0) \\ h_{2,\pm}(k_x, k_y, k_0) & 0 \end{pmatrix}, \quad (13)$$

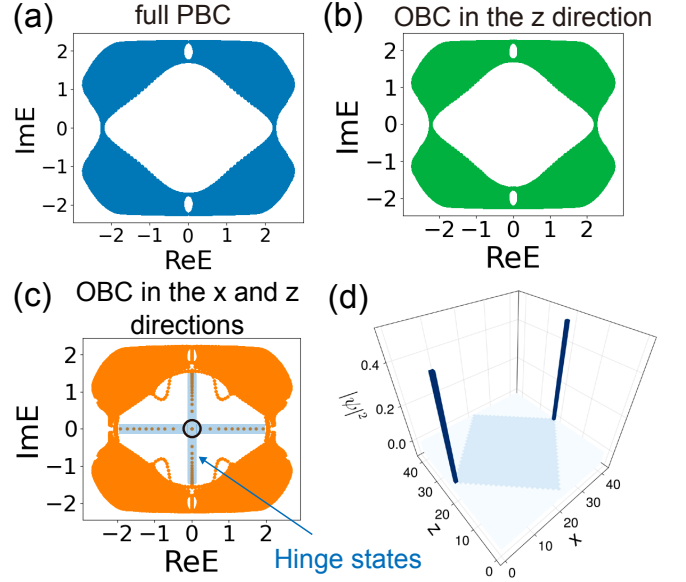


FIG. 3. (a-c) Complex energy spectra of the Hamiltonian (11) under the (a) full periodic boundary conditions (PBC), (b) open boundary conditions (OBC) in the z direction and PBC in the x and y directions, and (c) OBC in the x and z directions and PBC in the y direction. (d) Real-space distribution of one of the right eigenstates encircled by the circle in (c). The parameters are $t_1 = 0.4$ and $t_2 = 0.3$. The system size in the x direction is 40 in (c) and (d), and the number of layers is 81 in (b-d). The momentum resolutions in the k_i ($i = x, y$) direction are $\Delta k_i = 2\pi/80$ in the whole Brillouin zone in (b) and (c). For $-\pi/1000 \leq k_y \leq \pi/1000$, the momentum resolution is set to $\Delta k_y = 2\pi/40000$ to obtain the energy spectra of the hinge states.

and effectively reduces to quasi-2D systems in class AIII + \mathcal{S}_- . Their topological invariants are given by a pair of the Chern numbers of the Hermitian matrices $ih_{1,\pm}\sigma_z$ and $ih_{2,\pm}\sigma_z$: $(\text{Ch}_{\pm,1}, \text{Ch}_{\pm,2}) := (\text{Ch}[ih_{1,\pm}\sigma_z], \text{Ch}[ih_{2,\pm}\sigma_z])$ [27]. From these Chern numbers, we introduce the mirror Chern numbers

$$\text{Ch}_{\mathcal{M},i} = \frac{1}{2}(\text{Ch}_{+,i} - \text{Ch}_{-,i}), \quad (14)$$

with $i = 1, 2$. This result is consistent with the $\mathbb{Z} \oplus \mathbb{Z}$ classification for class AIII + \mathcal{S}_- in Table I. The pair of the mirror Chern numbers for our model takes $(\text{Ch}_{\mathcal{M},1}, \text{Ch}_{\mathcal{M},2}) = (1, 0)$ in the $k_z = \pi$ plane.

We calculate the energy spectra of Eq. (11) to obtain the boundary states corresponding to the nontrivial mirror Chern number for the point gap at $E = 0$ [Fig. 3(a)]. No boundary states are present under the OBC in the z direction and the PBC in both the x and y directions with the surface perpendicular to the z direction since reflection symmetry is not preserved [Fig. 3(b)]. By contrast, the hinge between the surfaces perpendicular to the $(1, 0, 1)$ and $(1, 0, -1)$ directions is invariant under the reflection, leading to the emergence of the bound-

ary states [Fig. 3(c)]. These boundary states are localized at the hinges that are invariant under the reflection $z \rightarrow -z$ [Fig. 3(d)]. Each hinge state supports a single EP, demonstrating that this 3D exceptional second-order topological insulator cannot be continuously deformed into Hermitian topological phases and hence is intrinsic to non-Hermitian systems. Notably, hinge states can appear even in the absence of sublattice symmetry, consistent with the \mathbb{Z} classification for class AIII with \mathcal{M}_+ in Table I. However, these hinge states are not necessarily intrinsic to non-Hermitian systems since they cannot support a single EP [92]. Furthermore, we show that this model exhibits an exotic surface state with two EPs that cannot be removed without breaking reflection symmetry also on surfaces perpendicular to the x direction (see Supplemental Material Sec. V [95]).

Summary. We develop classification of reflection-symmetric second-order point-gap topological phases. From this classification, we introduce 2D and 3D exceptional second-order topological insulators as distinct classes of point-gap topological phases with reflection symmetry and pseudo-reflection symmetry. 2D exceptional second-order topological insulators are feasible in metamaterials, such as photonic crystals, active matter, and electrical circuits, given the experimental realization of various point-gap topological phases in 2D systems [78–84]. While 3D point-gap topological phases have yet to be experimentally demonstrated, our layer construction approach offers a promising route for experimentally realizing 3D exceptional second-order topological insulators, based on the availability of 2D point-gap topological phases. Our findings thus expand the family of point-gap topological phases incorporating spatial symmetry.

Acknowledgments. D.N. and K.K. thank Ken Shiozaki for helpful discussion. D.N. thanks Masatoshi Sato for helpful discussion. We appreciate the long-term workshop “Recent Developments and Challenges in Topological Phases” (YITP-T-24-03) held at Yukawa Institute for Theoretical Physics (YITP), Kyoto University. Y.T. is supported by RIKEN Special Postdoctoral Researchers Program and Japan Society for the Promotion of Science (JSPS) KAKENHI Grant No. 24K22868. Y.T. and D.N. are supported by JST CREST Grant No. JPMJCR19T2. D.N. is supported by JSPS KAKENHI Grant No. 24K22857. R.O. is supported by JSPS KAKENHI Grants No. 23K13033 and No. 24K00586. K.K. is supported by MEXT KAKENHI Grant-in-Aid for Transformative Research Areas A “Extreme Universe” No. 24H00945.

* yutaro.tanaka.ay@riken.jp

† daichi.nakamura@issp.u-tokyo.ac.jp

‡ okugawa@rs.tus.ac.jp

§ kawabata@issp.u-tokyo.ac.jp

- [1] M. Z. Hasan and C. L. Kane, Colloquium: Topological insulators, *Rev. Mod. Phys.* **82**, 3045 (2010).
- [2] X.-L. Qi and S.-C. Zhang, Topological insulators and superconductors, *Rev. Mod. Phys.* **83**, 1057 (2011).
- [3] M. Sitte, A. Rosch, E. Altman, and L. Fritz, Topological Insulators in Magnetic Fields: Quantum Hall Effect and Edge Channels with a Nonquantized θ Term, *Phys. Rev. Lett.* **108**, 126807 (2012).
- [4] F. Zhang, C. L. Kane, and E. J. Mele, Surface State Magnetization and Chiral Edge States on Topological Insulators, *Phys. Rev. Lett.* **110**, 046404 (2013).
- [5] W. A. Benalcazar, B. A. Bernevig, and T. L. Hughes, Quantized electric multipole insulators, *Science* **357**, 61 (2017).
- [6] W. A. Benalcazar, B. A. Bernevig, and T. L. Hughes, Electric multipole moments, topological multipole moment pumping, and chiral hinge states in crystalline insulators, *Phys. Rev. B* **96**, 245115 (2017).
- [7] J. Langbehn, Y. Peng, L. Trifunovic, F. von Oppen, and P. W. Brouwer, Reflection-Symmetric Second-Order Topological Insulators and Superconductors, *Phys. Rev. Lett.* **119**, 246401 (2017).
- [8] Z. Song, Z. Fang, and C. Fang, $(d - 2)$ -Dimensional Edge States of Rotation Symmetry Protected Topological States, *Phys. Rev. Lett.* **119**, 246402 (2017).
- [9] F. Schindler, A. M. Cook, M. G. Vergniory, Z. Wang, S. S. Parkin, B. A. Bernevig, and T. Neupert, Higher-order topological insulators, *Sci. Adv.* **4**, eaat0346 (2018).
- [10] C. Fang and L. Fu, New classes of topological crystalline insulators having surface rotation anomaly, *Sci. Adv.* **5**, eaat2374 (2019).
- [11] G. Gamow, Zur Quantentheorie des Atomkernes, *Z. Physik* **51**, 204 (1928).
- [12] A. J. F. Siegert, On the Derivation of the Dispersion Formula for Nuclear Reactions, *Phys. Rev.* **56**, 750 (1939).
- [13] H. Feshbach, Unified theory of nuclear reactions, *Ann. Phys.* **5**, 357 (1958).
- [14] H. Feshbach, A unified theory of nuclear reactions. II, *Ann. Phys.* **19**, 287 (1962).
- [15] C. L. Kane and T. C. Lubensky, Topological boundary modes in isostatic lattices, *Nat. Phys.* **10**, 39 (2014).
- [16] S. D. Huber, Topological mechanics, *Nat. Phys.* **12**, 621 (2016).
- [17] V. V. Konotop, J. Yang, and D. A. Zezyulin, Nonlinear waves in \mathcal{PT} -symmetric systems, *Rev. Mod. Phys.* **88**, 035002 (2016).
- [18] L. Feng, R. El-Ganainy, and L. Ge, Non-Hermitian photonics based on parity–time symmetry, *Nat. Photon.* **11**, 752 (2017).
- [19] R. El-Ganainy, K. G. Makris, M. Khajavikhan, Z. H. Musslimani, S. Rotter, and D. N. Christodoulides, Non-Hermitian physics and PT symmetry, *Nat. Phys.* **14**, 11 (2018).
- [20] V. Kozii and L. Fu, Non-Hermitian topological theory of finite-lifetime quasiparticles: Prediction of bulk Fermi arc due to exceptional point, *Phys. Rev. B* **109**, 235139 (2024).
- [21] H. Shen and L. Fu, Quantum Oscillation from In-Gap States and a Non-Hermitian Landau Level Problem, *Phys. Rev. Lett.* **121**, 026403 (2018).
- [22] M. Papaj, H. Isobe, and L. Fu, Nodal arc of disordered

- Dirac fermions and non-Hermitian band theory, *Phys. Rev. B* **99**, 201107(R) (2019).
- [23] Y. Ashida, Z. Gong, and M. Ueda, Non-Hermitian physics, *Adv. Phys.* **69**, 249 (2020).
- [24] E. J. Bergholtz, J. C. Budich, and F. K. Kunst, Exceptional topology of non-Hermitian systems, *Rev. Mod. Phys.* **93**, 015005 (2021).
- [25] H. Shen, B. Zhen, and L. Fu, Topological Band Theory for Non-Hermitian Hamiltonians, *Phys. Rev. Lett.* **120**, 146402 (2018).
- [26] Z. Gong, Y. Ashida, K. Kawabata, K. Takasan, S. Higashikawa, and M. Ueda, Topological Phases of Non-Hermitian Systems, *Phys. Rev. X* **8**, 031079 (2018).
- [27] K. Kawabata, K. Shiozaki, M. Ueda, and M. Sato, Symmetry and Topology in Non-Hermitian Physics, *Phys. Rev. X* **9**, 041015 (2019).
- [28] T. E. Lee, Anomalous Edge State in a Non-Hermitian Lattice, *Phys. Rev. Lett.* **116**, 133903 (2016).
- [29] V. M. Martinez Alvarez, J. E. Barrios Vargas, and L. E. F. Foa Torres, Non-Hermitian robust edge states in one dimension: Anomalous localization and eigenspace condensation at exceptional points, *Phys. Rev. B* **97**, 121401(R) (2018).
- [30] S. Yao and Z. Wang, Edge States and Topological Invariants of Non-Hermitian Systems, *Phys. Rev. Lett.* **121**, 086803 (2018).
- [31] S. Yao, F. Song, and Z. Wang, Non-Hermitian Chern Bands, *Phys. Rev. Lett.* **121**, 136802 (2018).
- [32] F. K. Kunst, E. Edvardsson, J. C. Budich, and E. J. Bergholtz, Biorthogonal Bulk-Boundary Correspondence in Non-Hermitian Systems, *Phys. Rev. Lett.* **121**, 026808 (2018).
- [33] C. H. Lee and R. Thomale, Anatomy of skin modes and topology in non-Hermitian systems, *Phys. Rev. B* **99**, 201103(R) (2019).
- [34] H. Zhou and J. Y. Lee, Periodic table for topological bands with non-Hermitian symmetries, *Phys. Rev. B* **99**, 235112 (2019).
- [35] C. H. Lee, L. Li, and J. Gong, Hybrid Higher-Order Skin-Topological Modes in Nonreciprocal Systems, *Phys. Rev. Lett.* **123**, 016805 (2019).
- [36] K. Yokomizo and S. Murakami, Non-Bloch Band Theory of Non-Hermitian Systems, *Phys. Rev. Lett.* **123**, 066404 (2019).
- [37] F. Song, S. Yao, and Z. Wang, Non-Hermitian Skin Effect and Chiral Damping in Open Quantum Systems, *Phys. Rev. Lett.* **123**, 170401 (2019).
- [38] F. Song, S. Yao, and Z. Wang, Non-Hermitian Topological Invariants in Real Space, *Phys. Rev. Lett.* **123**, 246801 (2019).
- [39] S. Longhi, Probing non-Hermitian skin effect and non-Bloch phase transitions, *Phys. Rev. Res.* **1**, 023013 (2019).
- [40] D. S. Borgnia, A. J. Kruchkov, and R.-J. Slager, Non-Hermitian Boundary Modes and Topology, *Phys. Rev. Lett.* **124**, 056802 (2020).
- [41] N. Okuma, K. Kawabata, K. Shiozaki, and M. Sato, Topological Origin of Non-Hermitian Skin Effects, *Phys. Rev. Lett.* **124**, 086801 (2020).
- [42] K. Kawabata, N. Okuma, and M. Sato, Non-Bloch band theory of non-Hermitian Hamiltonians in the symplectic class, *Phys. Rev. B* **101**, 195147 (2020).
- [43] K. Zhang, Z. Yang, and C. Fang, Correspondence between Winding Numbers and Skin Modes in Non-Hermitian Systems, *Phys. Rev. Lett.* **125**, 126402 (2020).
- [44] T. Yoshida, T. Mizoguchi, and Y. Hatsugai, Mirror skin effect and its electric circuit simulation, *Phys. Rev. Res.* **2**, 022062(R) (2020).
- [45] K. Yokomizo and S. Murakami, Non-Bloch band theory in bosonic Bogoliubov-de Gennes systems, *Phys. Rev. B* **103**, 165123 (2021).
- [46] K. Yokomizo and S. Murakami, Scaling rule for the critical non-Hermitian skin effect, *Phys. Rev. B* **104**, 165117 (2021).
- [47] Y.-X. Xiao and C. T. Chan, Topology in non-Hermitian Chern insulators with skin effect, *Phys. Rev. B* **105**, 075128 (2022).
- [48] K. Yokomizo, T. Yoda, and S. Murakami, Non-Hermitian waves in a continuous periodic model and application to photonic crystals, *Phys. Rev. Res.* **4**, 023089 (2022).
- [49] K. Deng and B. Flebus, Non-Hermitian skin effect in magnetic systems, *Phys. Rev. B* **105**, L180406 (2022).
- [50] S. Longhi, Non-Hermitian skin effect and self-acceleration, *Phys. Rev. B* **105**, 245143 (2022).
- [51] Q. Liang, D. Xie, Z. Dong, H. Li, H. Li, B. Gadway, W. Yi, and B. Yan, Dynamic Signatures of Non-Hermitian Skin Effect and Topology in Ultracold Atoms, *Phys. Rev. Lett.* **129**, 070401 (2022).
- [52] S. Franca, V. Könye, F. Hassler, J. van den Brink, and C. Fulga, Non-Hermitian Physics without Gain or Loss: The Skin Effect of Reflected Waves, *Phys. Rev. Lett.* **129**, 086601 (2022).
- [53] K. Zhang, Z. Yang, and C. Fang, Universal non-Hermitian skin effect in two and higher dimensions, *Nat. Commun.* **13**, 2496 (2022).
- [54] Y. Jin, W. Zhong, R. Cai, X. Zhuang, Y. Pennec, and B. Djafari-Rouhani, Non-Hermitian skin effect in a phononic beam based on piezoelectric feedback control, *Appl. Phys. Lett.* **121**, 022202 (2022).
- [55] F. Alsallom, L. Herviou, O. V. Yazyev, and M. Brzezińska, Fate of the non-Hermitian skin effect in many-body fermionic systems, *Phys. Rev. Res.* **4**, 033122 (2022).
- [56] K. Kawabata, T. Numasawa, and S. Ryu, Entanglement Phase Transition Induced by the Non-Hermitian Skin Effect, *Phys. Rev. X* **13**, 021007 (2023).
- [57] Y. Tanaka, R. Takahashi, and R. Okugawa, Non-Hermitian skin effect enforced by nonsymmorphic symmetries, *Phys. Rev. B* **109**, 035131 (2024).
- [58] Y. O. Nakai, N. Okuma, D. Nakamura, K. Shimomura, and M. Sato, Topological enhancement of nonnormality in non-Hermitian skin effects, *Phys. Rev. B* **109**, 144203 (2024).
- [59] K. Shimomura and M. Sato, General Criterion for Non-Hermitian Skin Effects and Application: Fock Space Skin Effects in Many-Body Systems, *Phys. Rev. Lett.* **133**, 136502 (2024).
- [60] R. Peters and T. Yoshida, Hinge non-Hermitian skin effect in the single-particle properties of a strongly correlated f -electron system, *Phys. Rev. B* **110**, 125114 (2024).
- [61] S. Ishikawa and T. Yoshida, Non-Hermitian \mathbb{Z}_4 skin effect protected by glide symmetry, *Phys. Rev. B* **110**, 115301 (2024).
- [62] K. Kawabata, M. Sato, and K. Shiozaki, Higher-order non-Hermitian skin effect, *Phys. Rev. B* **102**, 205118 (2020).

- (2020).
- [63] R. Okugawa, R. Takahashi, and K. Yokomizo, Second-order topological non-Hermitian skin effects, *Phys. Rev. B* **102**, 241202(R) (2020).
 - [64] Y. Fu, J. Hu, and S. Wan, Non-Hermitian second-order skin and topological modes, *Phys. Rev. B* **103**, 045420 (2021).
 - [65] R. Okugawa, R. Takahashi, and K. Yokomizo, Non-Hermitian band topology with generalized inversion symmetry, *Phys. Rev. B* **103**, 205205 (2021).
 - [66] K. Shiozaki and S. Ono, Symmetry indicator in non-Hermitian systems, *Phys. Rev. B* **104**, 035424 (2021).
 - [67] C.-A. Li, B. Trauzettel, T. Neupert, and S.-B. Zhang, Enhancement of Second-Order Non-Hermitian Skin Effect by Magnetic Fields, *Phys. Rev. Lett.* **131**, 116601 (2023).
 - [68] C.-H. Liu, H. Hu, S. Chen, and X.-J. Liu, Anomalous second-order skin modes in Floquet non-Hermitian systems, *Phys. Rev. B* **108**, 174307 (2023).
 - [69] X.-Q. Sun, P. Zhu, and T. L. Hughes, Geometric Response and Disclination-Induced Skin Effects in Non-Hermitian Systems, *Phys. Rev. Lett.* **127**, 066401 (2021).
 - [70] F. Schindler and A. Prem, Dislocation non-Hermitian skin effect, *Phys. Rev. B* **104**, L161106 (2021).
 - [71] B. A. Bhargava, I. C. Fulga, J. van den Brink, and A. G. Moghaddam, Non-Hermitian skin effect of dislocations and its topological origin, *Phys. Rev. B* **104**, L241402 (2021).
 - [72] L. Xiao, T. Deng, K. Wang, G. Zhu, Z. Wang, W. Yi, and P. Xue, Non-Hermitian bulk–boundary correspondence in quantum dynamics, *Nat. Phys.* **16**, 761 (2020).
 - [73] S. Weidemann, M. Kremer, T. Helbig, T. Hofmann, A. Stegmaier, M. Greiter, R. Thomale, and A. Szameit, Topological funneling of light, *Science* **368**, 311 (2020).
 - [74] T. Helbig, T. Hofmann, S. Imhof, M. Abdelghany, T. Kiessling, L. Molenkamp, C. Lee, A. Szameit, M. Greiter, and R. Thomale, Generalized bulk–boundary correspondence in non-Hermitian topoelectrical circuits, *Nat. Phys.* **16**, 747 (2020).
 - [75] M. Brandenbourger, X. Locsin, E. Lerner, and C. Coulais, Non-reciprocal robotic metamaterials, *Nat. Commun.* **10**, 4608 (2019).
 - [76] Y. Chen, X. Li, C. Scheibner, V. Vitelli, and G. Huang, Realization of active metamaterials with odd micropolar elasticity, *Nat. Commun.* **12**, 5935 (2021).
 - [77] L. Zhang, Y. Yang, Y. Ge, Y.-J. Guan, Q. Chen, Q. Yan, F. Chen, R. Xi, Y. Li, D. Jia, S.-Q. Yuan, H.-X. Sun, H. Chen, and B. Zhang, Acoustic non-Hermitian skin effect from twisted winding topology, *Nat. Commun.* **12**, 6297 (2021).
 - [78] T. Hofmann, T. Helbig, F. Schindler, N. Salgo, M. Brzezińska, M. Greiter, T. Kiessling, D. Wolf, A. Vollhardt, A. Kabaši, C. H. Lee, A. Bilušić, R. Thomale, and T. Neupert, Reciprocal skin effect and its realization in a topoelectrical circuit, *Phys. Rev. Res.* **2**, 023265 (2020).
 - [79] L. S. Palacios, S. Tchoumakov, M. Guix, I. Pagonabarraga, S. Sánchez, and A. G. Grushin, Guided accumulation of active particles by topological design of a second-order skin effect, *Nat. Commun.* **12**, 4691 (2021).
 - [80] C. Shang, S. Liu, R. Shao, P. Han, X. Zang, X. Zhang, K. N. Salama, W. Gao, C. H. Lee, R. Thomale, A. Manchon, S. Zhang, T. J. Cui, and U. Schwingenschlögl, Experimental Identification of the Second-Order Non-Hermitian Skin Effect with Physics-Graph-Informed Machine Learning, *Adv. Sci.* **9**, 2202922 (2022).
 - [81] J. Wu, R. Zheng, J. Liang, M. Ke, J. Lu, W. Deng, X. Huang, and Z. Liu, Spin-Dependent Localization of Helical Edge States in a Non-Hermitian Phononic Crystal, *Phys. Rev. Lett.* **133**, 126601 (2024).
 - [82] Y. Sun, X. Hou, T. Wan, F. Wang, S. Zhu, Z. Ruan, and Z. Yang, Photonic Floquet Skin-Topological Effect, *Phys. Rev. Lett.* **132**, 063804 (2024).
 - [83] G.-G. Liu, S. Mandal, P. Zhou, X. Xi, R. Banerjee, Y.-H. Hu, M. Wei, M. Wang, Q. Wang, Z. Gao, H. Chen, Y. Yang, Y. Chong, and B. Zhang, Localization of Chiral Edge States by the Non-Hermitian Skin Effect, *Phys. Rev. Lett.* **132**, 113802 (2024).
 - [84] J.-X. Zhong, P. F. de Castro, T. Lu, J. Kim, M. Oudich, J. Ji, L. Shi, K. Chen, J. Lu, Y. Jing, and W. A. Benalcazar, Higher-order Skin Effect through a Hermitian-non-Hermitian Correspondence and Its Observation in an Acoustic Kagome Lattice, [arXiv:2409.01516](https://arxiv.org/abs/2409.01516) (2024).
 - [85] F. Terrier and F. K. Kunst, Dissipative analog of four-dimensional quantum Hall physics, *Phys. Rev. Res.* **2**, 023364 (2020).
 - [86] K. Kawabata, K. Shiozaki, and S. Ryu, Topological Field Theory of Non-Hermitian Systems, *Phys. Rev. Lett.* **126**, 216405 (2021).
 - [87] M. M. Denner, A. Skurativska, F. Schindler, M. H. Fischer, R. Thomale, T. Bzdušek, and T. Neupert, Exceptional topological insulators, *Nat. Commun.* **12**, 5681 (2021).
 - [88] M. M. Denner, T. Neupert, and F. Schindler, Infernal and exceptional edge modes: non-Hermitian topology beyond the skin effect, *J. Phys. Mater.* **6**, 045006 (2023).
 - [89] F. Schindler, K. Gu, B. Lian, and K. Kawabata, Hermitian Bulk – Non-Hermitian Boundary Correspondence, *PRX Quantum* **4**, 030315 (2023).
 - [90] D. Nakamura, K. Inaka, N. Okuma, and M. Sato, Universal Platform of Point-Gap Topological Phases from Topological Materials, *Phys. Rev. Lett.* **131**, 256602 (2023).
 - [91] G. K. Dash, S. Bid, and M. Thakurathi, Floquet exceptional topological insulator, *Phys. Rev. B* **109**, 035418 (2024).
 - [92] D. Nakamura, T. Bessho, and M. Sato, Bulk-Boundary Correspondence in Point-Gap Topological Phases, *Phys. Rev. Lett.* **132**, 136401 (2024).
 - [93] S. Hamanaka, T. Yoshida, and K. Kawabata, Non-Hermitian Topology in Hermitian Topological Matter, [arXiv:2405.10015](https://arxiv.org/abs/2405.10015) (2024).
 - [94] M. Geier, L. Trifunovic, M. Hoskam, and P. W. Brouwer, Second-order topological insulators and superconductors with an order-two crystalline symmetry, *Phys. Rev. B* **97**, 205135 (2018).
 - [95] See Supplemental Material at URL for further details on the classification of reflection-symmetric second-order point-gap topology, continuous deformation of the two-dimensional exceptional second-order topological insulator phase into a Hermitian topological phase (or more generally, line-gap topological phase), boundary states of $H_{2D}^{(\pm)}(\mathbf{k})$, a three-dimensional exceptional second-order topological insulator protected by inversion symmetry, and a surface state of $H_M(\mathbf{k})$.
 - [96] I. C. Fulga, N. Avraham, H. Beidenkopf, and A. Stern,

- Coupled-layer description of topological crystalline insulators, [Phys. Rev. B **94**, 125405 \(2016\)](#).
- [97] M. Ezawa, Hourglass fermion surface states in stacked topological insulators with nonsymmorphic symmetry, [Phys. Rev. B **94**, 155148 \(2016\)](#).
 - [98] H. Song, S.-J. Huang, L. Fu, and M. Hermele, Topological Phases Protected by Point Group Symmetry, [Phys. Rev. X **7**, 011020 \(2017\)](#).
 - [99] S.-J. Huang, H. Song, Y.-P. Huang, and M. Hermele, Building crystalline topological phases from lower-dimensional states, [Phys. Rev. B **96**, 205106 \(2017\)](#).
 - [100] Z. Song, T. Zhang, Z. Fang, and C. Fang, Quantitative mappings between symmetry and topology in solids, [Nat. Commun. **9**, 3530 \(2018\)](#).
 - [101] L. Trifunovic and P. W. Brouwer, Higher-Order Bulk-Boundary Correspondence for Topological Crystalline Phases, [Phys. Rev. X **9**, 011012 \(2019\)](#).
 - [102] E. Khalaf, Higher-order topological insulators and superconductors protected by inversion symmetry, [Phys. Rev. B **97**, 205136 \(2018\)](#).
 - [103] S. Ono and H. Watanabe, Unified understanding of symmetry indicators for all internal symmetry classes, [Phys. Rev. B **98**, 115150 \(2018\)](#).
 - [104] A. Matsugatani and H. Watanabe, Connecting higher-order topological insulators to lower-dimensional topological insulators, [Phys. Rev. B **98**, 205129 \(2018\)](#).
 - [105] S. H. Kooi, G. van Miert, and C. Ortix, Inversion-symmetry protected chiral hinge states in stacks of doped quantum hall layers, [Phys. Rev. B **98**, 245102 \(2018\)](#).
 - [106] Y. Tanaka, R. Takahashi, T. Zhang, and S. Murakami, Theory of inversion- \mathbb{Z}_4 protected topological chiral hinge states and its applications to layered antiferromagnets, [Phys. Rev. Res. **2**, 043274 \(2020\)](#).

Supplemental Material for “Exceptional Second-Order Topological Insulators”

SI. CLASSIFICATION OF REFLECTION-SYMMETRIC SECOND-ORDER POINT-GAP TOPOLOGY

We develop a classification of reflection-symmetric second-order point-gap topology. We consider non-Hermitian Hamiltonians H in the 38-fold internal-symmetry classification [27] with additional reflection symmetry. Owing to non-Hermiticity, we consider two different types of reflection symmetry,

$$\mathcal{M}H\mathcal{M}^{-1} = H, \quad \mathcal{M}^2 = 1, \quad (\text{S1})$$

and

$$\tilde{\mathcal{M}}H^\dagger\tilde{\mathcal{M}}^{-1} = H, \quad \tilde{\mathcal{M}}^2 = 1, \quad (\text{S2})$$

with unitary operators \mathcal{M} and $\tilde{\mathcal{M}}$. We call the former reflection symmetry for non-Hermitian Hamiltonians and the latter pseudo-reflection symmetry, or equivalently, reflection symmetry[†], following the terminology in Ref. [27]. To capture point-gap topology, it is useful to introduce the Hermitized Hamiltonians \mathbf{H} by

$$\mathbf{H} := \begin{pmatrix} 0 & H \\ H^\dagger & 0 \end{pmatrix}. \quad (\text{S3})$$

Point-gap topology of the original non-Hermitian Hamiltonians H is reduced to topology of the Hermitized Hamiltonians \mathbf{H} , and vice versa. Furthermore, symmetry for H leads to symmetry for \mathbf{H} . Specifically, reflection symmetry in Eq. (S1) and pseudo-reflection symmetry in Eq. (S2) lead to the following symmetries represented by

$$\mathbf{M}\mathbf{H}\mathbf{M}^{-1} = \mathbf{H}, \quad \mathbf{M} := \begin{pmatrix} \mathcal{M} & 0 \\ 0 & \mathcal{M} \end{pmatrix}, \quad \mathbf{M}^2 = 1, \quad (\text{S4})$$

$$\mathbf{M}\mathbf{H}\mathbf{M}^{-1} = \mathbf{H}, \quad \mathbf{M} := \begin{pmatrix} 0 & \tilde{\mathcal{M}} \\ \tilde{\mathcal{M}} & 0 \end{pmatrix}, \quad \mathbf{M}^2 = 1, \quad (\text{S5})$$

respectively. Additionally, the Hermitized Hamiltonians \mathbf{H} by construction respect chiral symmetry

$$\Sigma\mathbf{H}\Sigma^{-1} = -\mathbf{H}, \quad \Sigma := \begin{pmatrix} 1 & 0 \\ 0 & -1 \end{pmatrix}. \quad (\text{S6})$$

For each symmetry class of non-Hermitian Hamiltonians H , we specify the relevant symmetry class of the Hermitized Hamiltonians \mathbf{H} . Then, from the classification of reflection-symmetric second-order topology in Ref. [7], corresponding to the extrinsic (or equivalently, termination-dependent) classification with locally broken reflection symmetry in Ref. [94], we further identify second-order point-gap topology for these symmetry classes. In some symmetry classes, blocks of \mathbf{H} respect reflection antisymmetry,

$$\bar{\mathbf{M}}\mathbf{H}\bar{\mathbf{M}}^{-1} = -\mathbf{H}, \quad \bar{\mathbf{M}}^2 = 1, \quad (\text{S7})$$

although we begin with reflection symmetry or pseudo-reflection symmetry for H . We summarize our classification for the complex Altland-Zirnbauer class in Table S1, real Altland-Zirnbauer class in Table S2, and real Altland-Zirnbauer[†] class in Table S3. The classification of the other remaining classes is left for future work. It should be noted that this classification includes both second-order skin effect and exceptional topological insulators. Some classes should be accompanied by second-order skin effect, in a similar manner to Refs. [62, 63]. By contrast, other classes correspond to second-order exceptional topological insulators studied in the present work, including two-dimensional class D + $\tilde{\mathcal{M}}_+$ (\mathbb{Z}_2 classification) and three-dimensional class AIII + $\mathcal{S}_- + \mathcal{M}_{++}$ ($\mathbb{Z} \oplus \mathbb{Z}$ classification). Below, we explicitly describe the identification of the relevant symmetry classes for representative cases.

A. Class AIII + $\mathcal{S}_\pm + \mathcal{M}_{\pm\pm}/\tilde{\mathcal{M}}_{\pm\pm}$

1. Reflection

As a prime example of the complex Altland-Zirnbauer class, we study class AIII + $\mathcal{S}_\pm + \mathcal{M}_{\pm\pm}$. By definition, non-Hermitian Hamiltonians H respect chiral symmetry and sublattice symmetry,

$$\Gamma H^\dagger \Gamma^{-1} = -H, \quad \Gamma^2 = 1, \quad (\text{S8})$$

$$\mathcal{S} H \mathcal{S}^{-1} = -H, \quad \mathcal{S}^2 = 1, \quad (\text{S9})$$

in addition to reflection symmetry in Eq. (S1). These symmetries are required to satisfy the algebra

$$\Gamma \mathcal{S} = \epsilon_{\Gamma\mathcal{S}} \mathcal{S} \Gamma, \quad \Gamma \mathcal{M} = \epsilon_{\Gamma\mathcal{M}} \mathcal{M} \Gamma, \quad \mathcal{S} \mathcal{M} = \epsilon_{\mathcal{S}\mathcal{M}} \mathcal{M} \mathcal{S} \quad (\epsilon_{\Gamma\mathcal{S}}, \epsilon_{\Gamma\mathcal{M}}, \epsilon_{\mathcal{S}\mathcal{M}} \in \{\pm 1\}). \quad (\text{S10})$$

Now, we introduce the Hermitized Hamiltonians \mathbf{H} in Eq. (S3), for which the above symmetries are represented by

$$\Gamma \mathbf{H} \Gamma^{-1} = -\mathbf{H}, \quad \Gamma := \begin{pmatrix} 0 & \Gamma \\ \Gamma & 0 \end{pmatrix}, \quad \Gamma^2 = 1, \quad (\text{S11})$$

$$\mathcal{S} \mathbf{H} \mathcal{S}^{-1} = -\mathbf{H}, \quad \mathcal{S} := \begin{pmatrix} \mathcal{S} & 0 \\ 0 & \mathcal{S} \end{pmatrix}, \quad \mathcal{S}^2 = 1, \quad (\text{S12})$$

and Eq. (S4), with

$$\Gamma \mathcal{S} = \epsilon_{\Gamma\mathcal{S}} \mathcal{S} \Gamma, \quad \Gamma \mathcal{M} = \epsilon_{\Gamma\mathcal{M}} \mathcal{M} \Gamma, \quad \mathcal{S} \mathcal{M} = \epsilon_{\mathcal{S}\mathcal{M}} \mathcal{M} \mathcal{S}. \quad (\text{S13})$$

By construction, the Hermitized Hamiltonians \mathbf{H} respect additional chiral symmetry Σ in Eq. (S6), satisfying

$$\Gamma \Sigma = -\Sigma \Gamma, \quad \mathcal{S} \Sigma = \Sigma \mathcal{S}, \quad \mathcal{M} \Sigma = \Sigma \mathcal{M}. \quad (\text{S14})$$

Because of the simultaneous presence of the two chiral symmetries described by \mathcal{S} and Σ , the combined operation gives unitary symmetry that commutes with \mathbf{H} :

$$(\Sigma \mathcal{S}) \mathbf{H} (\Sigma \mathcal{S})^{-1} = \mathbf{H}, \quad (\Sigma \mathcal{S})^2 = 1. \quad (\text{S15})$$

Consequently, the Hermitized Hamiltonians \mathbf{H} can be block-diagonalized. This unitary symmetry is related to the other symmetries given by

$$\Gamma (\Sigma \mathcal{S}) = -\epsilon_{\Gamma\mathcal{S}} (\Sigma \mathcal{S}) \Gamma, \quad \mathcal{S} (\Sigma \mathcal{S}) = +(\Sigma \mathcal{S}) \mathcal{S}, \quad \Sigma (\Sigma \mathcal{S}) = +(\Sigma \mathcal{S}) \Sigma, \quad \mathcal{M} (\Sigma \mathcal{S}) = +\epsilon_{\mathcal{S}\mathcal{M}} (\Sigma \mathcal{S}) \mathcal{M}. \quad (\text{S16})$$

- $\epsilon_{\Gamma\mathcal{S}} = +1$ (class AIII + $\mathcal{S}_+ + \mathcal{M}_{\pm\pm}$).—While each block of \mathbf{H} respects chiral symmetry \mathcal{S} , it no longer respects chiral symmetry Γ . Therefore, the blocks belong to class AIII. Furthermore, for $\epsilon_{\mathcal{S}\mathcal{M}} = +1$, reflection symmetry \mathcal{M} is respected, and its commutation or anticommutation relation with chiral symmetry \mathcal{S} is specified by $\epsilon_{\mathcal{S}\mathcal{M}} = +1$. On the other hand, for $\epsilon_{\mathcal{S}\mathcal{M}} = -1$, reflection antisymmetry $\Gamma \mathcal{M}$ ($i\Gamma \mathcal{M}$) is respected for $\epsilon_{\Gamma\mathcal{M}} = +1$ ($\epsilon_{\Gamma\mathcal{M}} = -1$), and its commutation or anticommutation relation with chiral symmetry \mathcal{S} is specified by $\epsilon_{\Gamma\mathcal{S}} \epsilon_{\mathcal{S}\mathcal{M}} = -1$.
- $\epsilon_{\Gamma\mathcal{S}} = -1$ (class AIII + $\mathcal{S}_- + \mathcal{M}_{\pm\pm}$).—Each block of \mathbf{H} respects both chiral symmetries \mathcal{S} and Γ . Then, the combination of \mathcal{S} and Γ further gives unitary symmetry that commutes with \mathbf{H} :

$$(i\mathcal{S}\Gamma) \mathbf{H} (i\mathcal{S}\Gamma)^{-1} = \mathbf{H}, \quad (i\mathcal{S}\Gamma)^2 = 1. \quad (\text{S17})$$

The algebra between this unitary symmetry and the other symmetries is given by

$$\Gamma (i\mathcal{S}\Gamma) = -(i\mathcal{S}\Gamma) \Gamma, \quad \mathcal{S} (i\mathcal{S}\Gamma) = -(i\mathcal{S}\Gamma) \mathcal{S}, \quad \mathcal{M} (i\mathcal{S}\Gamma) = +\epsilon_{\Gamma\mathcal{M}} \epsilon_{\mathcal{S}\mathcal{M}} (i\mathcal{S}\Gamma) \mathcal{M}. \quad (\text{S18})$$

Each block diagonalized by the two unitary symmetries $\Sigma \mathcal{S}$ and $i\mathcal{S}\Gamma$ respects no internal symmetry and thus belongs to class A. Moreover, for $\epsilon_{\mathcal{S}\mathcal{M}} = +1$, reflection symmetry \mathcal{M} (antisymmetry $i\Gamma \mathcal{M}$) survives in each of the blocks for $\epsilon_{\Gamma\mathcal{M}} = +1$ ($\epsilon_{\Gamma\mathcal{M}} = -1$). For $\epsilon_{\mathcal{S}\mathcal{M}} = -1$, on the other hand, each block of $i\mathcal{S}\Gamma$ respects unitary symmetry $\Sigma \mathcal{S}$ and reflection symmetry \mathcal{M} that anticommute with each other, specified by “A + U + \mathcal{M}_- ” in Table S1.

2. Pseudo-reflection

We also study class AIII + $\mathcal{S}_\pm + \tilde{\mathcal{M}}_{\pm\pm}$. Non-Hermitian Hamiltonians H respect chiral symmetry in Eq. (S8), sublattice symmetry in Eq. (S9), and pseudo-reflection symmetry (or equivalently, reflection symmetry[†]) in Eq. (S2), satisfying

$$\Gamma \mathcal{S} = \epsilon_{\Gamma \mathcal{S}} \mathcal{S} \Gamma, \quad \Gamma \tilde{\mathcal{M}} = \epsilon_{\Gamma \tilde{\mathcal{M}}} \tilde{\mathcal{M}} \Gamma, \quad \mathcal{S} \tilde{\mathcal{M}} = \epsilon_{\mathcal{S} \tilde{\mathcal{M}}} \tilde{\mathcal{M}} \mathcal{S} \quad (\epsilon_{\Gamma \mathcal{S}}, \epsilon_{\Gamma \tilde{\mathcal{M}}}, \epsilon_{\mathcal{S} \tilde{\mathcal{M}}} \in \{\pm 1\}). \quad (\text{S19})$$

Correspondingly, the Hermitized Hamiltonians \mathbf{H} in Eq. (S3) respect Eqs. (S11), (S12), and (S5), with

$$\Gamma \mathbf{S} = \epsilon_{\Gamma \mathbf{S}} \mathbf{S} \Gamma, \quad \Gamma \mathbf{M} = \epsilon_{\Gamma \mathbf{M}} \mathbf{M} \Gamma, \quad \mathbf{S} \mathbf{M} = \epsilon_{\mathbf{S} \mathbf{M}} \mathbf{M} \mathbf{S}. \quad (\text{S20})$$

The additional chiral symmetry Σ in Eq. (S6) satisfies

$$\Gamma \Sigma = -\Sigma \Gamma, \quad \mathbf{S} \Sigma = \Sigma \mathbf{S}, \quad \mathbf{M} \Sigma = -\Sigma \mathbf{M}. \quad (\text{S21})$$

In a similar manner to Sec. SIA 1, \mathbf{H} is block-diagonalized by the unitary symmetry $\mathbf{S} \Sigma$ as in Eq. (S15), satisfying

$$\Gamma (\mathbf{S} \Sigma) = -\epsilon_{\Gamma \mathbf{S}} (\mathbf{S} \Sigma) \Gamma, \quad \mathbf{S} (\mathbf{S} \Sigma) = + (\mathbf{S} \Sigma) \mathbf{S}, \quad \Sigma (\mathbf{S} \Sigma) = + (\mathbf{S} \Sigma) \Sigma, \quad \mathbf{M} (\mathbf{S} \Sigma) = -\epsilon_{\mathbf{S} \mathbf{M}} (\mathbf{S} \Sigma) \mathbf{M}. \quad (\text{S22})$$

- $\epsilon_{\Gamma \mathbf{S}} = +1$ (class AIII + $\mathcal{S}_+ + \tilde{\mathcal{M}}_{\pm\pm}$).—While each block of \mathbf{H} respects chiral symmetry \mathbf{S} , it no longer respects chiral symmetry Γ . Therefore, the blocks belong to class AIII. For $\epsilon_{\mathbf{S} \mathbf{M}} = +1$, reflection antisymmetry $\Gamma \mathbf{M}$ ($i\Gamma \mathbf{M}$) is respected for $\epsilon_{\Gamma \mathbf{M}} = +1$ ($\epsilon_{\Gamma \mathbf{M}} = -1$), and its commutation or anticommutation relation with chiral symmetry \mathbf{S} is specified by $\epsilon_{\Gamma \mathbf{S}} \epsilon_{\mathbf{S} \mathbf{M}} = +1$. On the other hand, for $\epsilon_{\mathbf{S} \mathbf{M}} = -1$, reflection symmetry is respected, and its commutation or anticommutation relation with chiral symmetry \mathbf{S} is specified by $\epsilon_{\mathbf{S} \mathbf{M}} = -1$.
- $\epsilon_{\Gamma \mathbf{S}} = -1$ (class AIII + $\mathcal{S}_- + \tilde{\mathcal{M}}_{\pm\pm}$).—Each block of \mathbf{H} respects both chiral symmetries \mathbf{S} and Γ . Then, the combination of \mathbf{S} and Γ further gives unitary symmetry that commutes with \mathbf{H} :

$$(i\mathbf{S}\Gamma) \mathbf{H} (i\mathbf{S}\Gamma)^{-1} = \mathbf{H}, \quad (i\mathbf{S}\Gamma)^2 = 1. \quad (\text{S23})$$

The algebra between this unitary symmetry and the other symmetries is given by

$$\Gamma (i\mathbf{S}\Gamma) = - (i\mathbf{S}\Gamma) \Gamma, \quad \mathbf{S} (i\mathbf{S}\Gamma) = - (i\mathbf{S}\Gamma) \mathbf{S}, \quad \mathbf{M} (i\mathbf{S}\Gamma) = +\epsilon_{\Gamma \mathbf{M}} \epsilon_{\mathbf{S} \mathbf{M}} (i\mathbf{S}\Gamma) \mathbf{M}. \quad (\text{S24})$$

Each block diagonalized by the two unitary symmetries $\mathbf{S} \Sigma$ and $i\mathbf{S}\Gamma$ respects no internal symmetry and thus belongs to class A. Moreover, for $\epsilon_{\mathbf{S} \mathbf{M}} = -1$, reflection symmetry \mathbf{M} (antisymmetry $i\Gamma \mathbf{M}$) survives in each of the blocks for $\epsilon_{\Gamma \mathbf{M}} = -1$ ($\epsilon_{\Gamma \mathbf{M}} = +1$). For $\epsilon_{\mathbf{S} \mathbf{M}} = +1$, on the other hand, each block of $i\mathbf{S}\Gamma$ respects unitary symmetry $\mathbf{S} \Sigma$ and reflection symmetry \mathbf{M} that anticommute with each other, specified by “A + U + M₋” in Table S1.

B. Class BDI + $\mathcal{M}_{\pm\pm}/\tilde{\mathcal{M}}_{\pm\pm}$

1. Reflection

As a prime example of the real Altland-Zirnbauer class, we study class BDI + $\mathcal{M}_{\pm\pm}$. By definition, non-Hermitian Hamiltonians H respect time-reversal symmetry and particle-hole symmetry,

$$\mathcal{T} H^* \mathcal{T}^{-1} = H, \quad \mathcal{T} \mathcal{T}^* = +1, \quad (\text{S25})$$

$$\mathcal{C} H^T \mathcal{C}^{-1} = -H, \quad \mathcal{C} \mathcal{C}^* = +1, \quad (\text{S26})$$

in addition to reflection symmetry in Eq. (S1). These symmetries are required to respect

$$\mathcal{T} \mathcal{C}^* = \mathcal{C} \mathcal{T}^*, \quad \mathcal{T} \mathcal{M}^* = \epsilon_{\mathbf{T} \mathbf{M}} \mathcal{M} \mathcal{T}, \quad \mathcal{C} \mathcal{M}^* = \epsilon_{\mathbf{C} \mathbf{M}} \mathcal{M} \mathcal{C} \quad (\epsilon_{\mathbf{T} \mathbf{M}}, \epsilon_{\mathbf{C} \mathbf{M}} \in \{\pm 1\}). \quad (\text{S27})$$

As a consequence of these symmetries, the Hermitized Hamiltonians \mathbf{H} in Eq. (S3) respect

$$\mathbf{T} \mathbf{H}^* \mathbf{T}^{-1} = \mathbf{H}, \quad \mathbf{T} := \begin{pmatrix} \mathcal{T} & 0 \\ 0 & \mathcal{T} \end{pmatrix}, \quad \mathbf{T} \mathbf{T}^* = +1, \quad (\text{S28})$$

$$\mathbf{C} \mathbf{H}^T \mathbf{C}^{-1} = -\mathbf{H}, \quad \mathbf{C} := \begin{pmatrix} 0 & \mathcal{C} \\ \mathcal{C} & 0 \end{pmatrix}, \quad \mathbf{C} \mathbf{C}^* = +1, \quad (\text{S29})$$

and Eq. (S4) with

$$\mathcal{T}\mathcal{C}^* = \mathcal{C}\mathcal{T}^*, \quad \mathcal{T}\mathcal{M}^* = \epsilon_{\text{TM}}\mathcal{M}\mathcal{T}, \quad \mathcal{C}\mathcal{M}^* = \epsilon_{\text{CM}}\mathcal{M}\mathcal{C}. \quad (\text{S30})$$

By construction, the Hermitized Hamiltonians \mathcal{H} respect additional chiral symmetry Σ in Eq. (S6), which satisfies

$$\mathcal{T}\Sigma^* = \Sigma\mathcal{T}, \quad \mathcal{C}\Sigma^* = -\Sigma\mathcal{C}, \quad \mathcal{M}\Sigma = \Sigma\mathcal{M}. \quad (\text{S31})$$

Because of the simultaneous presence of the two independent chiral symmetries specified by $i\mathcal{T}\mathcal{C}^*$ and Σ , their combination gives unitary symmetry that commutes with \mathcal{H} :

$$(i\mathcal{T}\mathcal{C}^*\Sigma)\mathcal{H}(i\mathcal{T}\mathcal{C}^*\Sigma)^{-1} = \mathcal{H}, \quad (i\mathcal{T}\mathcal{C}^*\Sigma)^2 = 1. \quad (\text{S32})$$

The algebra between this unitary symmetry and the other symmetries is given by

$$\begin{aligned} \mathcal{T}(i\mathcal{T}\mathcal{C}^*\Sigma)^* &= -(i\mathcal{T}\mathcal{C}^*\Sigma)\mathcal{T}, & \mathcal{C}(i\mathcal{T}\mathcal{C}^*\Sigma)^* &= +(i\mathcal{T}\mathcal{C}^*\Sigma)\mathcal{C}, \\ \Sigma(i\mathcal{T}\mathcal{C}^*\Sigma) &= -(i\mathcal{T}\mathcal{C}^*\Sigma)\Sigma, & \mathcal{M}(i\mathcal{T}\mathcal{C}^*\Sigma) &= \epsilon_{\text{TM}}\epsilon_{\text{CM}}(i\mathcal{T}\mathcal{C}^*\Sigma)\mathcal{M}. \end{aligned} \quad (\text{S33})$$

Thus, each block of \mathcal{H} only respects particle-hole symmetry \mathcal{C} and belongs to class D. The presence of reflection symmetry or antisymmetry in the blocks depends on $\epsilon_{\text{TM}}\epsilon_{\text{CM}}$, as follows:

- $\epsilon_{\text{TM}}\epsilon_{\text{CM}} = +1$.—Reflection symmetry \mathcal{M} is respected, and its commutation or anticommutation relation with particle-hole symmetry \mathcal{C} is specified by ϵ_{CM} .
- $\epsilon_{\text{TM}}\epsilon_{\text{CM}} = -1$.—Reflection antisymmetry $\mathcal{M}\Sigma$ is respected, and its commutation or anticommutation relation with particle-hole symmetry \mathcal{C} is specified by $-\epsilon_{\text{CM}}$.

2. Pseudo-reflection

We next consider class BDI + $\tilde{\mathcal{M}}_{\pm\pm}$. Non-Hermitian Hamiltonians \mathcal{H} respect time-reversal symmetry in Eq. (S25), particle-hole symmetry in Eq. (S26), and pseudo-reflection symmetry (or equivalently, reflection symmetry[†]) in Eq. (S2), satisfying

$$\mathcal{T}\mathcal{C}^* = \mathcal{C}\mathcal{T}^*, \quad \mathcal{T}\tilde{\mathcal{M}}^* = \epsilon_{\text{TM}}\tilde{\mathcal{M}}\mathcal{T}, \quad \mathcal{C}\tilde{\mathcal{M}}^* = \epsilon_{\text{CM}}\tilde{\mathcal{M}}\mathcal{C} \quad (\epsilon_{\text{TM}}, \epsilon_{\text{CM}} \in \{\pm 1\}). \quad (\text{S34})$$

As a consequence, the Hermitized Hamiltonians \mathcal{H} in Eq. (S3) respect Eqs. (S28), (S29), and (S5), with

$$\mathcal{T}\mathcal{C}^* = \mathcal{C}\mathcal{T}^*, \quad \mathcal{T}\mathcal{M}^* = \epsilon_{\text{TM}}\mathcal{M}\mathcal{T}, \quad \mathcal{C}\mathcal{M}^* = \epsilon_{\text{CM}}\mathcal{M}\mathcal{C}. \quad (\text{S35})$$

The additional chiral symmetry Σ in Eq. (S6) satisfies

$$\mathcal{T}\Sigma^* = \Sigma\mathcal{T}, \quad \mathcal{C}\Sigma^* = -\Sigma\mathcal{C}, \quad \mathcal{M}\Sigma = -\Sigma\mathcal{M}. \quad (\text{S36})$$

Similarly to Sec. SIB 1, \mathcal{H} is block-diagonalized by the unitary symmetry $i\mathcal{T}\mathcal{C}^*\Sigma$ as in Eq. (S32), satisfying

$$\begin{aligned} \mathcal{T}(i\mathcal{T}\mathcal{C}^*\Sigma)^* &= -(i\mathcal{T}\mathcal{C}^*\Sigma)\mathcal{T}, & \mathcal{C}(i\mathcal{T}\mathcal{C}^*\Sigma)^* &= +(i\mathcal{T}\mathcal{C}^*\Sigma)\mathcal{C}, \\ \Sigma(i\mathcal{T}\mathcal{C}^*\Sigma) &= -(i\mathcal{T}\mathcal{C}^*\Sigma)\Sigma, & \mathcal{M}(i\mathcal{T}\mathcal{C}^*\Sigma) &= -\epsilon_{\text{TM}}\epsilon_{\text{CM}}(i\mathcal{T}\mathcal{C}^*\Sigma)\mathcal{M}. \end{aligned} \quad (\text{S37})$$

Thus, each block of \mathcal{H} only respects particle-hole symmetry \mathcal{C} and belongs to class D. The presence of reflection symmetry or antisymmetry in the blocks depends on $\epsilon_{\text{TM}}\epsilon_{\text{CM}}$, as follows:

- $\epsilon_{\text{TM}}\epsilon_{\text{CM}} = +1$.—Reflection antisymmetry $i\mathcal{M}\Sigma$ is respected, and its commutation or anticommutation relation with particle-hole symmetry \mathcal{C} is specified by ϵ_{CM} .
- $\epsilon_{\text{TM}}\epsilon_{\text{CM}} = -1$.—Reflection symmetry \mathcal{M} is respected, and its commutation or anticommutation relation with particle-hole symmetry \mathcal{C} is specified by ϵ_{CM} .

C. Class $\text{DIII}^\dagger + \mathcal{M}_{\pm\pm}/\tilde{\mathcal{M}}_{\pm\pm}$

1. Reflection

As a prime example of the real Altland-Zirnbauer[†] class, we study class $\text{DIII}^\dagger + \mathcal{M}_{\pm\pm}$. Non-Hermitian Hamiltonians H respect time-reversal symmetry[†] and particle-hole symmetry[†],

$$\mathcal{T}H^T\mathcal{T}^{-1} = H, \quad \mathcal{T}\mathcal{T}^* = -1, \quad (\text{S38})$$

$$\mathcal{C}H^*\mathcal{C}^{-1} = -H, \quad \mathcal{C}\mathcal{C}^* = +1, \quad (\text{S39})$$

in addition to reflection symmetry in Eq. (S1). These symmetries are required to respect

$$\mathcal{T}\mathcal{C}^* = -\mathcal{C}\mathcal{T}^*, \quad \mathcal{T}\mathcal{M}^* = \epsilon_{\text{TM}}\mathcal{M}\mathcal{T}, \quad \mathcal{C}\mathcal{M}^* = \epsilon_{\text{CM}}\mathcal{M}\mathcal{C} \quad (\epsilon_{\text{TM}}, \epsilon_{\text{CM}} \in \{\pm 1\}). \quad (\text{S40})$$

As a consequence of these symmetries, the Hermitized Hamiltonians \mathbf{H} in Eq. (S3) respect

$$\mathbf{T}\mathbf{H}^T\mathbf{T}^{-1} = \mathbf{H}, \quad \mathbf{T} := \begin{pmatrix} 0 & \mathcal{T} \\ \mathcal{T} & 0 \end{pmatrix}, \quad \mathbf{T}\mathbf{T}^* = -1, \quad (\text{S41})$$

$$\mathbf{C}\mathbf{H}^*\mathbf{C}^{-1} = -\mathbf{H}, \quad \mathbf{C} := \begin{pmatrix} \mathcal{C} & 0 \\ 0 & \mathcal{C} \end{pmatrix}, \quad \mathbf{C}\mathbf{C}^* = +1, \quad (\text{S42})$$

and Eq. (S4), with

$$\mathbf{T}\mathbf{C}^* = -\mathbf{C}\mathbf{T}^*, \quad \mathbf{T}\mathbf{M}^* = \epsilon_{\text{TM}}\mathbf{M}\mathbf{T}, \quad \mathbf{C}\mathbf{M}^* = \epsilon_{\text{CM}}\mathbf{M}\mathbf{C}. \quad (\text{S43})$$

By construction, \mathbf{H} respects additional chiral symmetry Σ in Eq. (S6), satisfying

$$\mathbf{T}\Sigma^* = -\Sigma\mathbf{T}, \quad \mathbf{C}\Sigma^* = \Sigma\mathbf{C}, \quad \mathbf{M}\Sigma = \Sigma\mathbf{M}. \quad (\text{S44})$$

Because of the simultaneous presence of the two independent chiral symmetries specified by $i\mathbf{T}\mathbf{C}^*$ and Σ , their combination gives unitary symmetry that commutes with \mathbf{H} , as in Eq. (S32). The algebra between this unitary symmetry and the other symmetries also coincides with Eq. (S33). Thus, each block of \mathbf{H} only respects particle-hole symmetry \mathbf{C} and hence belongs to class D. The presence of reflection symmetry or antisymmetry in the blocks depends on $\epsilon_{\text{TM}}\epsilon_{\text{CM}}$, as follows:

- $\epsilon_{\text{TM}}\epsilon_{\text{CM}} = +1$.—Reflection symmetry \mathbf{M} is respected, and its commutation or anticommutation relation with particle-hole symmetry \mathbf{C} is specified by ϵ_{CM} .
- $\epsilon_{\text{TM}}\epsilon_{\text{CM}} = -1$.—Reflection antisymmetry $\mathbf{M}\Sigma$ is respected, and its commutation or anticommutation relation with particle-hole symmetry \mathbf{C} is specified by ϵ_{CM} .

2. Pseudo-reflection

We also study class $\text{DIII}^\dagger + \tilde{\mathcal{M}}_{\pm\pm}$. Non-Hermitian Hamiltonians H respect time-reversal symmetry[†] in Eq. (S38), particle-hole symmetry[†] in Eq. (S39), and pseudo-reflection symmetry (or equivalently, reflection symmetry[†]) in Eq. (S2), satisfying

$$\mathcal{T}\mathcal{C}^* = -\mathcal{C}\mathcal{T}^*, \quad \mathcal{T}\tilde{\mathcal{M}}^* = \epsilon_{\text{TM}}\tilde{\mathcal{M}}\mathcal{T}, \quad \mathcal{C}\tilde{\mathcal{M}}^* = \epsilon_{\text{CM}}\tilde{\mathcal{M}}\mathcal{C} \quad (\epsilon_{\text{TM}}, \epsilon_{\text{CM}} \in \{\pm 1\}). \quad (\text{S45})$$

The Hermitized Hamiltonian \mathbf{H} in Eq. (S3) respects Eqs. (S41), (S42), and (S5), with

$$\mathbf{T}\mathbf{C}^* = -\mathbf{C}\mathbf{T}^*, \quad \mathbf{T}\mathbf{M}^* = \epsilon_{\text{TM}}\mathbf{M}\mathbf{T}, \quad \mathbf{C}\mathbf{M}^* = \epsilon_{\text{CM}}\mathbf{M}\mathbf{C}. \quad (\text{S46})$$

The additional chiral symmetry Σ in Eq. (S6) satisfies

$$\mathbf{T}\Sigma^* = -\Sigma\mathbf{T}, \quad \mathbf{C}\Sigma^* = \Sigma\mathbf{C}, \quad \mathbf{M}\Sigma = -\Sigma\mathbf{M}. \quad (\text{S47})$$

Similarly to Sec. SIC 1, \mathbf{H} is block diagonalized by the unitary symmetry $i\mathbf{T}\mathbf{C}^*\Sigma$, as in Eq. (S32). The algebra between this unitary symmetry and the other symmetries also coincides with Eq. (S37). Thus, each block of \mathbf{H} only respects particle-hole symmetry \mathbf{C} and belongs to class D. The presence of reflection symmetry or antisymmetry in the blocks depends on $\epsilon_{\text{TM}}\epsilon_{\text{CM}}$, as follows:

- $\epsilon_{\text{TM}}\epsilon_{\text{CM}} = +1$.—Reflection antisymmetry $i\mathbf{M}\Sigma$ is respected, and its commutation or anticommutation relation with particle-hole symmetry \mathbf{C} is specified by $-\epsilon_{\text{CM}}$.
- $\epsilon_{\text{TM}}\epsilon_{\text{CM}} = -1$.—Reflection symmetry \mathbf{M} is respected, and its commutation or anticommutation relation with particle-hole symmetry \mathbf{C} is specified by ϵ_{CM} .

D. Boundary classification

While we have hitherto developed the bulk classification, direct analysis of second-order topological boundary states is also feasible. As illustrative cases, we here study Hermitian Hamiltonians in classes AIII + \mathbf{M}_+ , AIII + \mathbf{U}_+ + \mathbf{M}_{+-} , and AIII + \mathbf{U}_+ + \mathbf{M}_{+-} , all of which are included in Table S1.

1. Class AIII + \mathbf{M}_+

We investigate second-order topological boundary states of Hermitian systems in class AIII + \mathbf{M}_+ . We consider a Hermitian Hamiltonian $\mathbf{H}(k_i, \mathbf{k}_{\parallel})$ around a reflection-invariant corner or hinge, where k_i denotes momentum perpendicular to the mirror plane, and \mathbf{k}_{\parallel} momenta within the mirror plane. Then, $\mathbf{H}(k_i, \mathbf{k}_{\parallel})$ respects chiral symmetry and reflection symmetry that commute with each other:

$$\Gamma \mathbf{H}(k_i, \mathbf{k}_{\parallel}) \Gamma^{-1} = -\mathbf{H}(k_i, \mathbf{k}_{\parallel}), \quad \mathbf{M}_+ \mathbf{H}(k_i, \mathbf{k}_{\parallel}) \mathbf{M}_+^{-1} = \mathbf{H}(-k_i, \mathbf{k}_{\parallel}), \quad (\text{S48})$$

with unitary matrices Γ and \mathbf{M}_+ satisfying

$$\Gamma^2 = \mathbf{M}_+^2 = 1, \quad [\Gamma, \mathbf{M}_+] = 0. \quad (\text{S49})$$

Around a reflection-invariant corner in a two-dimensional system, a gapless state $\mathbf{H}(k_i) = k_i \sigma_x$ appears, where the symmetry operators are chosen as $\Gamma = \sigma_z$ and $\mathbf{M}_+ = \sigma_z$. On the other hand, away from the reflection-invariant corner, this gapless state is lifted by a perturbation $m\sigma_y$ ($m \in \mathbb{R}$). This demonstrates the emergence of corner states at zero energy, consistent with Table S1. By contrast, around a reflection-invariant hinge in a three-dimensional system, no symmetry-preserving gapless states appear, showing the absence of second-order topological boundary states.

2. Class AIII + \mathbf{U}_+ + \mathbf{M}_{+-}

In class AIII + \mathbf{U}_+ + \mathbf{M}_{+-} , a Hermitian Hamiltonian $\mathbf{H}(k_i, \mathbf{k}_{\parallel})$ around a reflection-invariant corner or hinge respects chiral symmetry, onsite unitary symmetry, and reflection symmetry,

$$\Gamma \mathbf{H}(k_i, \mathbf{k}_{\parallel}) \Gamma^{-1} = -\mathbf{H}(k_i, \mathbf{k}_{\parallel}), \quad \mathbf{U} \mathbf{H}(k_i, \mathbf{k}_{\parallel}) \mathbf{U}^{-1} = \mathbf{H}(k_i, \mathbf{k}_{\parallel}), \quad \mathbf{M}_{+-} \mathbf{H}(k_i, \mathbf{k}_{\parallel}) \mathbf{M}_{+-}^{-1} = \mathbf{H}(-k_i, \mathbf{k}_{\parallel}), \quad (\text{S50})$$

with unitary matrices Γ , \mathbf{U} , and \mathbf{M}_{+-} satisfying

$$\Gamma^2 = \mathbf{U}^2 = \mathbf{M}_{+-}^2 = 1, \quad [\Gamma, \mathbf{U}] = [\Gamma, \mathbf{M}_{+-}] = \{\mathbf{U}, \mathbf{M}_{+-}\} = 0. \quad (\text{S51})$$

For the choice of $\Gamma = \tau_z \sigma_0$, $\mathbf{U} = \tau_0 \sigma_z$, $\mathbf{M}_{+-} = \tau_z \sigma_x$, generic mass terms that preserve both the chiral and onsite unitary symmetries are given as $\tau_x \sigma_0$, $\tau_x \sigma_z$, $\tau_y \sigma_0$, $\tau_y \sigma_z$, two of which (i.e., $\tau_x \sigma_z$, $\tau_y \sigma_z$) are even under reflection, and the other two of which (i.e., $\tau_x \sigma_0$, $\tau_y \sigma_0$) are odd. Consequently, no gapless states appear around a reflection-invariant corner in a two-dimensional system. On the other hand, around a reflection-invariant hinge in a three-dimensional system, a first-order gapless surface state $\mathbf{H}(k_i, k_{\parallel}) = k_i \tau_x \sigma_0 + k_{\parallel} \tau_y \sigma_z$ appears, where the symmetry operators are chosen as $\Gamma = \tau_z \sigma_0$, $\mathbf{U} = \tau_0 \sigma_z$, $\mathbf{M}_{+-} = \tau_z \sigma_x$. To eliminate this first-order topology, we stack this surface state and obtain $\mathbf{H}(k_i, k_{\parallel}) = (k_i \tau_x \sigma_0 + k_{\parallel} \tau_y \sigma_z) \rho_z$ with $\Gamma = \tau_z \sigma_0 \rho_z$, $\mathbf{U} = \tau_0 \sigma_z \rho_0$, $\mathbf{M}_{+-} = \tau_z \sigma_x \rho_0$, where ρ_z is the Pauli matrix, and ρ_0 is the two-by-two identity matrix. In such a case, it can be gapped out by a symmetry-preserving mass term $m\rho_x$ ($m \in \mathbb{R}$), implying the absence of second-order topological boundary states.

3. Class $A + U + M_-$

In class $A + U + M_-$, a Hermitian Hamiltonian $H(k_i, \mathbf{k}_\parallel)$ around a reflection-invariant corner or hinge respects onsite unitary symmetry and reflection symmetry,

$$UH(k_i, \mathbf{k}_\parallel)U^{-1} = H(k_i, \mathbf{k}_\parallel), \quad M_-H(k_i, \mathbf{k}_\parallel)M_-^{-1} = H(-k_i, \mathbf{k}_\parallel), \quad (\text{S52})$$

with unitary matrices U and M_- satisfying

$$U^2 = M_-^2 = 1, \quad \{U, M_-\} = 0. \quad (\text{S53})$$

Around a reflection-invariant corner in a two-dimensional system, a first-order gapless edge state $H(k_i) = k_i\sigma_z$ appears, where the symmetry operators are chosen as $U = \sigma_z$ and $M_- = \sigma_x$. To eliminate this first-order topology, we stack this edge state, yielding $H(k_i) = k_i\tau_z\sigma_z$ with $U = \tau_0\sigma_z$ and $M_- = \tau_z\sigma_x$. In such a case, it can be gapped out by a symmetry-preserving mass term $m\tau_x\sigma_z$ ($m \in \mathbb{R}$). This implies the absence of second-order topological boundary states, consistent with Table S1. Additionally, around a reflection-invariant hinge in a three-dimensional system, no symmetry-preserving gapless states appear, showing the absence of second-order topological boundary states.

TABLE S1. Classification of second-order point-gap topology in the complex Altland-Zirnbauer symmetry classes with reflection symmetry. The subscript of \mathcal{S} specifies the commutation (+) or anticommutation (−) relation with chiral symmetry. \mathcal{M} and $\tilde{\mathcal{M}}$ denote reflection symmetry and pseudo-reflection symmetry (or equivalently, reflection symmetry[†]), respectively. In classes AIII and $A + \mathcal{S}$, the subscript of \mathcal{M}_{\pm} or $\tilde{\mathcal{M}}_{\pm}$ specifies the commutation (+) or anticommutation (−) relation with chiral and sublattice symmetries, respectively. In classes AIII + \mathcal{S}_{\pm} , the first subscript of $\mathcal{M}_{\pm\pm}$ or $\tilde{\mathcal{M}}_{\pm\pm}$ specifies the relation to chiral symmetry and the second one to sublattice symmetry.

Class	Hermitization	$d = 2$	$d = 3$
$A + \mathcal{M}$	AIII + \mathbf{M}_+	\mathbb{Z}	0
$A + \tilde{\mathcal{M}}$	AIII + \mathbf{M}_-	0	0
AIII + \mathcal{M}_+	$A + \mathbf{M}$	0	\mathbb{Z}
AIII + \mathcal{M}_-	$A + \bar{\mathbf{M}}$	0	0
AIII + $\tilde{\mathcal{M}}_+$	$A + \bar{\mathbf{M}}$	0	0
AIII + $\tilde{\mathcal{M}}_-$	$A + \mathbf{M}$	0	\mathbb{Z}
AIII + $\mathcal{S}_+ + \mathcal{M}_{++}$	AIII + \mathbf{M}_+	\mathbb{Z}	0
AIII + $\mathcal{S}_+ + \mathcal{M}_{+-}$	AIII + \mathbf{M}_-	0	0
AIII + $\mathcal{S}_+ + \mathcal{M}_{-+}$	AIII + \mathbf{M}_+	\mathbb{Z}	0
AIII + $\mathcal{S}_+ + \mathcal{M}_{--}$	AIII + \mathbf{M}_-	0	0
AIII + $\mathcal{S}_+ + \tilde{\mathcal{M}}_{++}$	AIII + \mathbf{M}_+	\mathbb{Z}	0
AIII + $\mathcal{S}_+ + \tilde{\mathcal{M}}_{+-}$	AIII + \mathbf{M}_-	0	0
AIII + $\mathcal{S}_+ + \tilde{\mathcal{M}}_{-+}$	AIII + \mathbf{M}_+	\mathbb{Z}	0
AIII + $\mathcal{S}_+ + \tilde{\mathcal{M}}_{--}$	AIII + \mathbf{M}_-	0	0
$A + \mathcal{S} + \mathcal{M}_+$	$(\text{AIII} + \mathbf{M}_+) \times (\text{AIII} + \mathbf{M}_+)$	$\mathbb{Z} \oplus \mathbb{Z}$	0
$A + \mathcal{S} + \mathcal{M}_-$	AIII + $\mathbf{U}_+ + \mathbf{M}_{+-}$	0	0
$A + \mathcal{S} + \tilde{\mathcal{M}}_+$	AIII + $\mathbf{U}_+ + \mathbf{M}_{+-}$	0	0
$A + \mathcal{S} + \tilde{\mathcal{M}}_-$	$(\text{AIII} + \mathbf{M}_-) \times (\text{AIII} + \mathbf{M}_-)$	0	0
AIII + $\mathcal{S}_- + \mathcal{M}_{++}$	$(A + \mathbf{M}) \times (A + \mathbf{M})$	0	$\mathbb{Z} \oplus \mathbb{Z}$
AIII + $\mathcal{S}_- + \mathcal{M}_{+-}$	$A + \mathbf{U} + \mathbf{M}_-$	0	0
AIII + $\mathcal{S}_- + \mathcal{M}_{-+}$	$(A + \bar{\mathbf{M}}) \times (A + \bar{\mathbf{M}})$	0	0
AIII + $\mathcal{S}_- + \mathcal{M}_{--}$	$A + \mathbf{U} + \mathbf{M}_-$	0	0
AIII + $\mathcal{S}_- + \tilde{\mathcal{M}}_{++}$	$A + \mathbf{U} + \mathbf{M}_-$	0	0
AIII + $\mathcal{S}_- + \tilde{\mathcal{M}}_{+-}$	$(A + \bar{\mathbf{M}}) \times (A + \bar{\mathbf{M}})$	0	0
AIII + $\mathcal{S}_- + \tilde{\mathcal{M}}_{-+}$	$A + \mathbf{U} + \mathbf{M}_-$	0	0
AIII + $\mathcal{S}_- + \tilde{\mathcal{M}}_{--}$	$(A + \mathbf{M}) \times (A + \mathbf{M})$	0	$\mathbb{Z} \oplus \mathbb{Z}$

TABLE S2. Classification of second-order point-gap topology in the real Altland-Zirnbauer symmetry classes with reflection symmetry. \mathcal{M} and $\tilde{\mathcal{M}}$ denote reflection symmetry and pseudo-reflection symmetry (or equivalently, reflection symmetry[†]), respectively. The subscript of \mathcal{M}_{\pm} or $\tilde{\mathcal{M}}_{\pm}$ specifies the commutation (+) or anticommutation (−) relation to time-reversal symmetry or particle-hole symmetry. For the symmetry classes involving both time-reversal symmetry and particle-hole symmetry (i.e., classes BDI, DIII, CII, and CI), the first subscript of $\mathcal{M}_{\pm\pm}$ or $\tilde{\mathcal{M}}_{\pm\pm}$ specifies the relation to time-reversal symmetry and the second one to particle-hole symmetry.

Class	Hermitization	$d = 2$	$d = 3$
AI + \mathcal{M}_+	BDI + \mathbf{M}_{++}	\mathbb{Z}	0
AI + \mathcal{M}_-	BDI + \mathbf{M}_{--}	$2\mathbb{Z}$	0
AI + $\tilde{\mathcal{M}}_+$	BDI + \mathbf{M}_{+-}	0	0
AI + $\tilde{\mathcal{M}}_-$	BDI + \mathbf{M}_{-+}	0	0
BDI + \mathcal{M}_{++}	D + \mathbf{M}_+	\mathbb{Z}_2	\mathbb{Z}
BDI + \mathcal{M}_{+-}	D + $\bar{\mathbf{M}}_+$	\mathbb{Z}_2	0
BDI + \mathcal{M}_{-+}	D + $\bar{\mathbf{M}}_-$	0	0
BDI + \mathcal{M}_{--}	D + \mathbf{M}_-	0	$2\mathbb{Z}$
BDI + $\tilde{\mathcal{M}}_{++}$	D + $\bar{\mathbf{M}}_+$	\mathbb{Z}_2	0
BDI + $\tilde{\mathcal{M}}_{+-}$	D + \mathbf{M}_-	0	$2\mathbb{Z}$
BDI + $\tilde{\mathcal{M}}_{-+}$	D + \mathbf{M}_+	\mathbb{Z}_2	\mathbb{Z}
BDI + $\tilde{\mathcal{M}}_{--}$	D + $\bar{\mathbf{M}}_-$	0	0
D + \mathcal{M}_+	DIII + \mathbf{M}_{++}	\mathbb{Z}_2	\mathbb{Z}_2
D + \mathcal{M}_-	DIII + \mathbf{M}_{--}	\mathbb{Z}_2	0
D + $\tilde{\mathcal{M}}_+$	DIII + \mathbf{M}_{-+}	\mathbb{Z}_2	\mathbb{Z}_2
D + $\tilde{\mathcal{M}}_-$	DIII + \mathbf{M}_{+-}	0	0
DIII + \mathcal{M}_{++}	AII + \mathbf{M}_+	0	\mathbb{Z}_2
DIII + \mathcal{M}_{+-}	AII + $\bar{\mathbf{M}}_+$	0	0
DIII + \mathcal{M}_{-+}	AII + $\bar{\mathbf{M}}_-$	0	\mathbb{Z}_2
DIII + \mathcal{M}_{--}	AII + \mathbf{M}_-	0	\mathbb{Z}_2
DIII + $\tilde{\mathcal{M}}_{++}$	AII + $\bar{\mathbf{M}}_-$	0	\mathbb{Z}_2
DIII + $\tilde{\mathcal{M}}_{+-}$	AII + \mathbf{M}_+	0	\mathbb{Z}_2
DIII + $\tilde{\mathcal{M}}_{-+}$	AII + \mathbf{M}_-	0	\mathbb{Z}_2
DIII + $\tilde{\mathcal{M}}_{--}$	AII + $\bar{\mathbf{M}}_+$	0	0
AII + \mathcal{M}_+	CII + \mathbf{M}_{++}	$2\mathbb{Z}$	0
AII + \mathcal{M}_-	CII + \mathbf{M}_{--}	$2\mathbb{Z}$	0
AII + $\tilde{\mathcal{M}}_+$	CII + \mathbf{M}_{+-}	0	0
AII + $\tilde{\mathcal{M}}_-$	CII + \mathbf{M}_{-+}	0	0
CII + \mathcal{M}_{++}	C + \mathbf{M}_+	0	$2\mathbb{Z}$
CII + \mathcal{M}_{+-}	C + $\bar{\mathbf{M}}_+$	0	0
CII + \mathcal{M}_{-+}	C + $\bar{\mathbf{M}}_-$	0	0
CII + \mathcal{M}_{--}	C + \mathbf{M}_-	0	$2\mathbb{Z}$
CII + $\tilde{\mathcal{M}}_{++}$	C + $\bar{\mathbf{M}}_+$	0	0
CII + $\tilde{\mathcal{M}}_{+-}$	C + \mathbf{M}_-	0	$2\mathbb{Z}$
CII + $\tilde{\mathcal{M}}_{-+}$	C + \mathbf{M}_+	0	$2\mathbb{Z}$
CII + $\tilde{\mathcal{M}}_{--}$	C + $\bar{\mathbf{M}}_-$	0	0
C + \mathcal{M}_+	CI + \mathbf{M}_{++}	0	0
C + \mathcal{M}_-	CI + \mathbf{M}_{--}	0	0
C + $\tilde{\mathcal{M}}_+$	CI + \mathbf{M}_{-+}	0	0
C + $\tilde{\mathcal{M}}_-$	CI + \mathbf{M}_{+-}	0	0
CI + \mathcal{M}_{++}	AI + \mathbf{M}_+	0	0
CI + \mathcal{M}_{+-}	AI + $\bar{\mathbf{M}}_+$	0	0
CI + \mathcal{M}_{-+}	AI + $\bar{\mathbf{M}}_-$	0	0
CI + \mathcal{M}_{--}	AI + \mathbf{M}_-	0	0
CI + $\tilde{\mathcal{M}}_{++}$	AI + $\bar{\mathbf{M}}_-$	0	0
CI + $\tilde{\mathcal{M}}_{+-}$	AI + \mathbf{M}_+	0	0
CI + $\tilde{\mathcal{M}}_{-+}$	AI + \mathbf{M}_-	0	0
CI + $\tilde{\mathcal{M}}_{--}$	AI + $\bar{\mathbf{M}}_+$	0	0

TABLE S3. Classification of second-order point-gap topology in the real Altland-Zirnbauer[†] symmetry classes with reflection symmetry. \mathcal{M} and $\tilde{\mathcal{M}}$ denote reflection symmetry and pseudo-reflection symmetry (or equivalently, reflection symmetry[†]), respectively. The subscript of \mathcal{M}_{\pm} or $\tilde{\mathcal{M}}_{\pm}$ specifies the commutation (+) or anticommutation (−) relation to time-reversal symmetry[†] or particle-hole symmetry[†]. For the symmetry classes involving both time-reversal symmetry[†] and particle-hole symmetry[†] (i.e., classes BDI[†], DIII[†], CII[†], and CI[†]), the first subscript of $\mathcal{M}_{\pm\pm}$ or $\tilde{\mathcal{M}}_{\pm\pm}$ specifies the relation to time-reversal symmetry[†] and the second one to particle-hole symmetry[†].

Class	Hermitization	$d = 2$	$d = 3$
AI [†] + \mathcal{M}_+	CI + \mathbf{M}_{++}	0	0
AI [†] + \mathcal{M}_-	CI + \mathbf{M}_{--}	0	0
AI [†] + $\tilde{\mathcal{M}}_+$	CI + \mathbf{M}_{+-}	0	0
AI [†] + $\tilde{\mathcal{M}}_-$	CI + \mathbf{M}_{-+}	0	0
BDI [†] + \mathcal{M}_{++}	AI + \mathbf{M}_+	0	0
BDI [†] + \mathcal{M}_{+-}	AI + $\bar{\mathbf{M}}_-$	0	0
BDI [†] + \mathcal{M}_{-+}	AI + $\bar{\mathbf{M}}_+$	0	0
BDI [†] + \mathcal{M}_{--}	AI + \mathbf{M}_-	0	0
BDI [†] + $\tilde{\mathcal{M}}_{++}$	AI + $\bar{\mathbf{M}}_+$	0	0
BDI [†] + $\tilde{\mathcal{M}}_{+-}$	AI + \mathbf{M}_+	0	0
BDI [†] + $\tilde{\mathcal{M}}_{-+}$	AI + \mathbf{M}_-	0	0
BDI [†] + $\tilde{\mathcal{M}}_{--}$	AI + $\bar{\mathbf{M}}_-$	0	0
D [†] + \mathcal{M}_+	BDI + \mathbf{M}_{++}	\mathbb{Z}	0
D [†] + \mathcal{M}_-	BDI + \mathbf{M}_{--}	$2\mathbb{Z}$	0
D [†] + $\tilde{\mathcal{M}}_+$	BDI + \mathbf{M}_{-+}	0	0
D [†] + $\tilde{\mathcal{M}}_-$	BDI + \mathbf{M}_{+-}	0	0
DIII [†] + \mathcal{M}_{++}	D + \mathbf{M}_+	\mathbb{Z}_2	\mathbb{Z}
DIII [†] + \mathcal{M}_{+-}	D + $\bar{\mathbf{M}}_-$	0	0
DIII [†] + \mathcal{M}_{-+}	D + $\bar{\mathbf{M}}_+$	\mathbb{Z}_2	0
DIII [†] + \mathcal{M}_{--}	D + \mathbf{M}_-	0	$2\mathbb{Z}$
DIII [†] + $\tilde{\mathcal{M}}_{++}$	D + $\bar{\mathbf{M}}_-$	0	0
DIII [†] + $\tilde{\mathcal{M}}_{+-}$	D + \mathbf{M}_-	0	$2\mathbb{Z}$
DIII [†] + $\tilde{\mathcal{M}}_{-+}$	D + \mathbf{M}_+	\mathbb{Z}_2	\mathbb{Z}
DIII [†] + $\tilde{\mathcal{M}}_{--}$	D + $\bar{\mathbf{M}}_+$	\mathbb{Z}_2	0
AII [†] + \mathcal{M}_+	DIII + \mathbf{M}_{++}	\mathbb{Z}_2	\mathbb{Z}_2
AII [†] + \mathcal{M}_-	DIII + \mathbf{M}_{--}	\mathbb{Z}_2	0
AII [†] + $\tilde{\mathcal{M}}_+$	DIII + \mathbf{M}_{+-}	0	0
AII [†] + $\tilde{\mathcal{M}}_-$	DIII + \mathbf{M}_{-+}	\mathbb{Z}_2	\mathbb{Z}_2
CII [†] + \mathcal{M}_{++}	AII + \mathbf{M}_+	0	\mathbb{Z}_2
CII [†] + \mathcal{M}_{+-}	AII + $\bar{\mathbf{M}}_-$	0	\mathbb{Z}_2
CII [†] + \mathcal{M}_{-+}	AII + $\bar{\mathbf{M}}_+$	0	0
CII [†] + \mathcal{M}_{--}	AII + \mathbf{M}_-	0	\mathbb{Z}_2
CII [†] + $\tilde{\mathcal{M}}_{++}$	AII + $\bar{\mathbf{M}}_+$	0	0
CII [†] + $\tilde{\mathcal{M}}_{+-}$	AII + \mathbf{M}_+	0	\mathbb{Z}_2
CII [†] + $\tilde{\mathcal{M}}_{-+}$	AII + \mathbf{M}_-	0	\mathbb{Z}_2
CII [†] + $\tilde{\mathcal{M}}_{--}$	AII + $\bar{\mathbf{M}}_-$	0	\mathbb{Z}_2
C [†] + \mathcal{M}_+	CII + \mathbf{M}_{++}	$2\mathbb{Z}$	0
C [†] + \mathcal{M}_-	CII + \mathbf{M}_{--}	$2\mathbb{Z}$	0
C [†] + $\tilde{\mathcal{M}}_+$	CII + \mathbf{M}_{-+}	0	0
C [†] + $\tilde{\mathcal{M}}_-$	CII + \mathbf{M}_{+-}	0	0
CI [†] + \mathcal{M}_{++}	C + \mathbf{M}_+	0	$2\mathbb{Z}$
CI [†] + \mathcal{M}_{+-}	C + $\bar{\mathbf{M}}_-$	0	0
CI [†] + \mathcal{M}_{-+}	C + $\bar{\mathbf{M}}_+$	0	0
CI [†] + \mathcal{M}_{--}	C + \mathbf{M}_-	0	$2\mathbb{Z}$
CI [†] + $\tilde{\mathcal{M}}_{++}$	C + $\bar{\mathbf{M}}_-$	0	0
CI [†] + $\tilde{\mathcal{M}}_{+-}$	C + \mathbf{M}_-	0	$2\mathbb{Z}$
CI [†] + $\tilde{\mathcal{M}}_{-+}$	C + \mathbf{M}_+	0	$2\mathbb{Z}$
CI [†] + $\tilde{\mathcal{M}}_{--}$	C + $\bar{\mathbf{M}}_+$	0	0

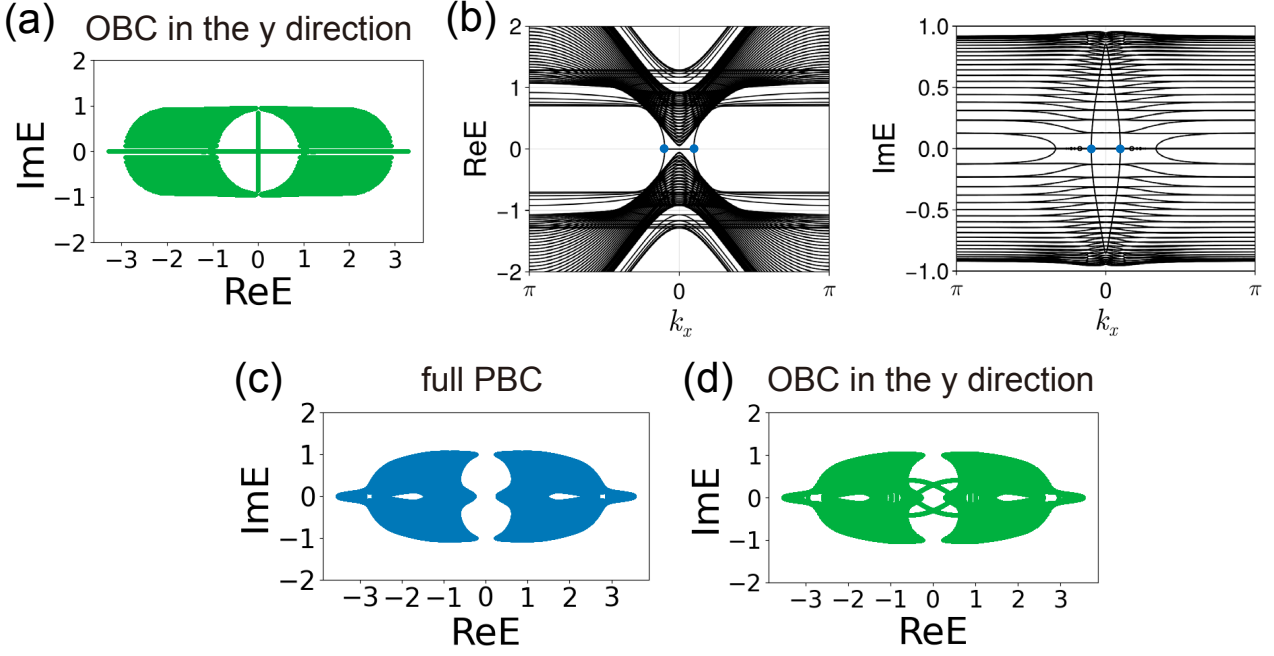


FIG. S1. (a) Complex energy spectra of the Hamiltonian $H_{\tilde{\mathcal{M}}}(\mathbf{k})$ in Eq. (6) in the main text with $m_1 = 0.1$ and $m_2 = 0.3$ under the open boundary conditions (OBC) in the y direction. (b) Energy dispersion of $H_{\tilde{\mathcal{M}}}(\mathbf{k})$. The blue points indicate the exceptional points. (c,d) Energy spectra of $H'_{\tilde{\mathcal{M}}}(\mathbf{k})$ in Eq. (S54) with $m_1 = 0.1$, $m_2 = 0.3$, and $m_3 = m_4 = 0.5$ under the (c) full periodic boundary conditions (PBC) and (d) OBC in the y direction and PBC in the x direction. The system size is 51 in the y direction with the momentum resolution $\Delta k_x = 2\pi/10000$.

SII. CONTINUOUS DEFORMATION INTO LINE-GAP TOPOLOGICAL PHASE

We show that the point-gap topological phase in $H_{\tilde{\mathcal{M}}}(\mathbf{k})$ introduced in Eq. (6) in the main text can be continuously deformed into a line-gap topological phase with respect to $\text{Re}E = 0$. We calculate the energy spectra of the Hamiltonian $H_{\tilde{\mathcal{M}}}(\mathbf{k})$ under the open boundary conditions (OBC) along the y direction [Fig. S1(a)]. Since the boundaries along the x axis are invariant under the reflection $x \rightarrow -x$, the boundary states are protected by pseudo-reflection symmetry. The boundary states support a pair of exceptional points [Fig. S1(b)], which is consistent with the continuum theory in terms of the effective Hamiltonian given by Eq. (5) in the main text.

Next, we add mass terms to the Hamiltonian $H_{\tilde{\mathcal{M}}}(\mathbf{k})$:

$$H'_{\tilde{\mathcal{M}}}(\mathbf{k}) = H_{\tilde{\mathcal{M}}}(\mathbf{k}) + im_3\sigma_y + im_4\tau_z\sigma_y. \quad (\text{S54})$$

These mass terms respect both particle-hole symmetry and pseudo-reflection symmetry, opening a line gap with respect to $\text{Re}E = 0$ [Fig. S1(c)]. The boundary states appear under the OBC in the y direction [Fig. S1(d)]. In the presence of the boundary states, the line gap at $\text{Re}E = 0$ closes. Thus, by adding appropriate mass terms, the exceptional second-order topological insulator can be continuously deformed into the line-gap topological phase.

SIII. 2D EXCEPTIONAL TOPOLOGICAL INSULATOR

We show that the Hamiltonian $H_{2\text{D}}^{(\pm)}(\mathbf{k})$ in Eq. (7) in the main text exhibits boundary states with a single exceptional point. The Hamiltonian $H_{2\text{D}}^{(\pm)}(\mathbf{k})$ respects chiral symmetry

$$\Gamma(H_{2\text{D}}^{(\pm)}(\mathbf{k}))^\dagger \Gamma^{-1} = -H_{2\text{D}}^{(\pm)}(\mathbf{k}), \quad \Gamma := \tau_x \gamma, \quad \gamma := \sigma_z, \quad (\text{S55})$$

and sublattice symmetry

$$\mathcal{S}H_{2\text{D}}^{(\pm)}(\mathbf{k})\mathcal{S}^{-1} = -H_{2\text{D}}^{(\pm)}(\mathbf{k}), \quad \mathcal{S} := \tau_z. \quad (\text{S56})$$

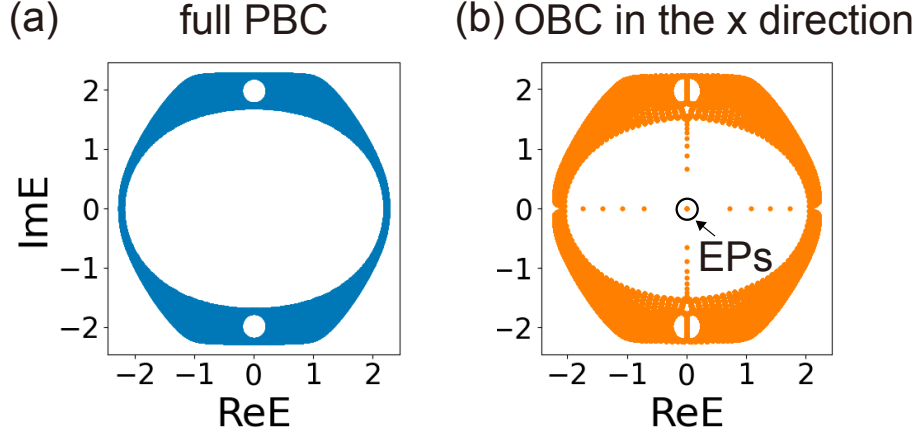


FIG. S2. Complex energy spectra of the 2D exceptional topological insulator $H_{2D}^{(+)}(\mathbf{k})$ under the (a) full periodic boundary conditions (PBC) and (b) open boundary conditions (OBC) in the x direction and PBC in the y direction. “EPs” indicates exceptional points. The system size in the x direction is 30, and the momentum resolution is $\Delta k_y = 2\pi/20000$ in (b). The parameters are the same as those in the main text.

The symmetry operators Γ and \mathcal{S} satisfy the anticommutation relation

$$\Gamma\mathcal{S} = -\mathcal{S}\Gamma. \quad (\text{S57})$$

Therefore, this model belongs to class AIII + \mathcal{S}_- in the 38-fold symmetry classification [27]. In this symmetry class, the non-Hermitian Hamiltonian $H_{2D}^{(\pm)}(\mathbf{k})$ satisfies

$$\mathcal{S}[i\Gamma H_{2D}^{(\pm)}(\mathbf{k})]\mathcal{S}^{-1} = i\Gamma H_{2D}^{(\pm)}(\mathbf{k}), \quad \mathcal{S}^2 = 1, \quad (\text{S58})$$

which implies that the Hermitian matrix $i\Gamma H_{2D}^{(\pm)}(\mathbf{k})$ can be block-diagonalized into the two Hermitian matrices labeled by the eigenvalues ± 1 of \mathcal{S} : $ih_1^{(\pm)}\gamma$ and $ih_2^{(\pm)}\gamma$. Topological invariants for these point-gap topological phases are given by a pair of the Chern numbers of the two Hermitian matrices $ih_1^{(\pm)}\gamma$ and $ih_2^{(\pm)}\gamma$ [27]:

$$(\text{Ch}_1, \text{Ch}_2) := (\text{Ch}[ih_1^{(\pm)}\gamma], \text{Ch}[ih_2^{(\pm)}\gamma]) \in \mathbb{Z} \oplus \mathbb{Z}. \quad (\text{S59})$$

When $(\text{Ch}_1, \text{Ch}_2) = (\pm 1, 0)$ or $(\text{Ch}_1, \text{Ch}_2) = (0, \pm 1)$ is satisfied, the system is a 2D exceptional topological insulator supporting edge states with a single exceptional point [88, 92].

The Hamiltonian $H_{2D}^{(+)}(\mathbf{k})$ has a point gap at $E = 0$ in the complex energy plane under the full periodic boundary conditions (PBC) [Fig. S2(a)]. The pair of the Chern numbers is given by $(\text{Ch}_1, \text{Ch}_2) = (1, 0)$, and the model has edge states under the OBC in the x direction [Fig. S2(b)]. These edge states host a single exceptional point, as discussed in the following.

A. Exceptional points

Here, we show the emergence of edge states with exceptional points in $H_{2D}^{(\pm)}$ in the main text, based on the discussion in Ref. [92]. Since our model $H_{2D}^{(\pm)}$ possesses sublattice symmetry with $\mathcal{S} = \tau_z$, the Hamiltonian is expressed as

$$H_{2D}^{(\pm)} = \begin{pmatrix} 0 & h_1^{(\pm)} \\ h_2^{(\pm)} & 0 \end{pmatrix}. \quad (\text{S60})$$

The matrix $h_1^{(\pm)}$ has a point gap at $E = 0$ in the full PBC [Fig. S3(a)] and hosts boundary states in the OBC in the x direction [Fig. S3(b)]. Consequently, $h_1^{(\pm)}$ has an eigenvector $|\psi_0\rangle$ with zero eigenvalue under the OBC in the x direction,

$$h_1^{(\pm)}|\psi_0\rangle = 0. \quad (\text{S61})$$

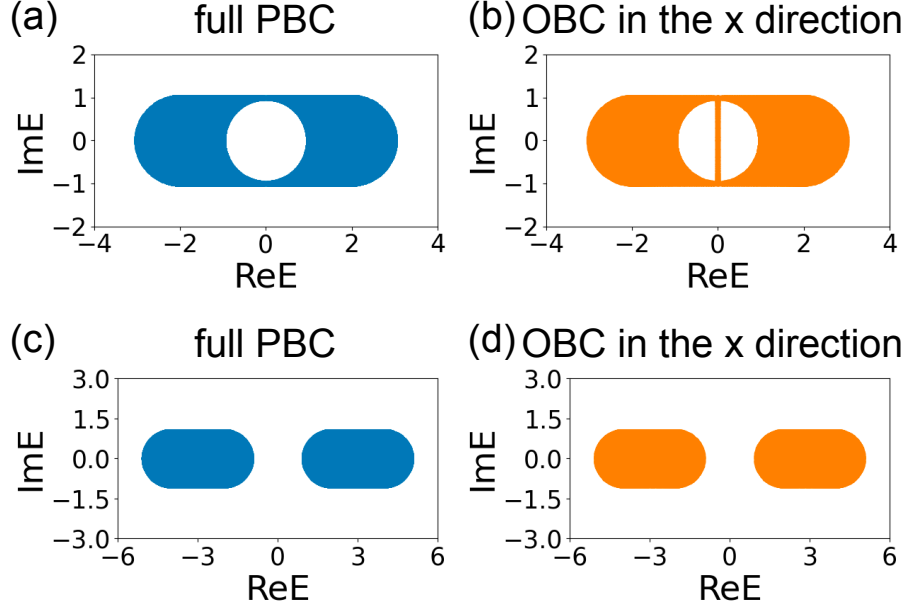


FIG. S3. Complex energy spectra of (a,b) $h_1^{(\pm)}(\mathbf{k})$ and (c,d) $h_2^{(\pm)}(\mathbf{k})$. (a,c) The boundary conditions are the full periodic boundary conditions (PBC). (b,d) The boundary conditions are the open boundary conditions (OBC) in the x direction and the PBC in the y direction. The parameters are the same as those in the main text. The system size is 50 in the x direction.

On the other hand, the matrix $h_2^{(\pm)}$ does not have a point gap to yield nontrivial topology [Fig. S3(c)] and therefore the system does not host boundary states [Fig. S3(d)]. Because $h_2^{(\pm)}$ does not have a zero eigenvalue, an inverse matrix $(h_2^{(\pm)})^{-1}$ exists.

Here, we introduce the following basis,

$$|\Psi_0^1\rangle := \begin{pmatrix} 0 \\ |\psi_0\rangle \end{pmatrix}, \quad |\Psi_0^2\rangle := \begin{pmatrix} (h_2^{(\pm)})^{-1} |\psi_0\rangle \\ 0 \end{pmatrix}, \quad (\text{S62})$$

and then we get

$$H_{2D}^{(\pm)} |\Psi_0^1\rangle = 0, \quad H_{2D}^{(\pm)} |\Psi_0^2\rangle = |\Psi_0^1\rangle. \quad (\text{S63})$$

We cannot introduce $|\Psi_0^1\rangle$ and $|\Psi_0^2\rangle$ under the full PBC because $h_1^{(\pm)}$ does not have $|\psi_0\rangle$ with a zero eigenvalue. Therefore, we find that the boundary states $|\psi_0\rangle$ of $h_1^{(\pm)}$ lead to the emergence of boundary states $|\Psi_0^1\rangle$ in $H_{2D}^{(\pm)}$. Furthermore, $H_{2D}^{(\pm)}$ has a Jordan block with zero diagonal components:

$$H_{2D}^{(\pm)} |\Psi_0^i\rangle = \sum_{j=1,2} |\Psi_0^j\rangle J_{ji}, \quad J := \begin{pmatrix} 0 & 1 \\ 0 & 0 \end{pmatrix}. \quad (\text{S64})$$

It follows that $H_{2D}^{(\pm)}$ hosts boundary states with exceptional points.

B. Energy dispersion and inversion-symmetry breaking

Here, we discuss the band dispersion of the 2D exceptional topological insulator $H_{2D}^{(+)}(\mathbf{k})$ and show that the boundary states possess an exceptional point. The Hamiltonian $H_{2D}^{(+)}(\mathbf{k})$ respects inversion symmetry

$$\mathcal{I} H_{2D}^{(\pm)}(\mathbf{k}) \mathcal{I}^{-1} = H_{2D}^{(\pm)}(-\mathbf{k}), \quad (\text{S65})$$

with $\mathcal{I} = \tau_z \sigma_y$. Figure S4(a) shows the band structure of $H_{2D}^{(+)}(\mathbf{k})$ in the k_y direction under the OBC in the x direction. The numerical result shows that the gapless states appear at $k_y = 0$ and support the exceptional point. In the following, we show that inversion-symmetry breaking leads to the square-root behavior of the exceptional point. We add an inversion-symmetry-breaking term,

$$\Delta H_{2D} = 0.5i \begin{pmatrix} 0 & 0 & 0 & 0 \\ 0 & 0 & 0 & 0 \\ 1 & 0 & 0 & 0 \\ 0 & 1 & 0 & 0 \end{pmatrix}, \quad (\text{S66})$$

to $H_{2D}^{(+)}(\mathbf{k})$. This term does not break sublattice or chiral symmetry, and does not close the point gap at $E = 0$. Therefore, the topological invariants are still given by $(\text{Ch}_1, \text{Ch}_2) = (1, 0)$, resulting in the emergence of boundary states that are topologically equivalent to those of $H_{2D}^{(+)}(\mathbf{k})$. Figure S4(b) shows that the energy dispersion of the boundary states of $H_{2D}^{(+)}(\mathbf{k}) + \Delta H_{2D}$ exhibits the square-root dependence on the wave vector.

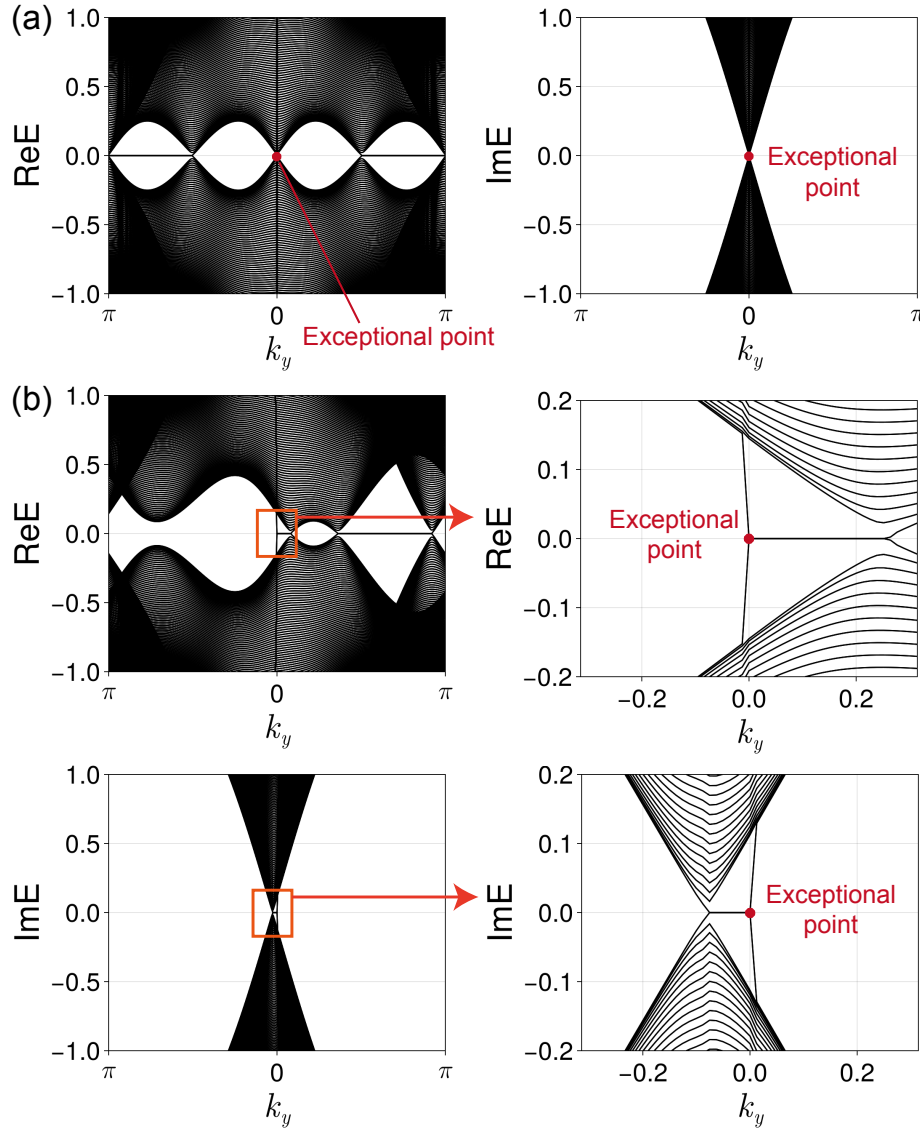


FIG. S4. Band structures of (a) $H_{2D}^{(+)}(\mathbf{k})$ and (b) $H_{2D}^{(+)}(\mathbf{k}) + \Delta H_{2D}$ under the open boundary conditions (OBC) in the x direction and the periodic boundary conditions (PBC) in the y direction. The system size is 200 in the x direction. The momentum resolution is $\Delta k_y = 2\pi/500$. The parameters of $H_{2D}^{(+)}(\mathbf{k})$ are the same as those in the main text.

SIV. 3D EXCEPTIONAL TOPOLOGICAL INSULATORS PROTECTED BY INVERSION SYMMETRY

We propose another 3D exceptional second-order topological insulator protected by inversion (parity) symmetry, which is different from the reflection-symmetric exceptional second-order topological insulator in the main text. We construct this 3D exceptional second-order topological insulator, using the layer construction in a similar manner to reflection-symmetric one in the main text. We introduce the 2D exceptional topological insulators $H_{2D}^{(+)}(\mathbf{k})$ and $H_{2D}^{(-)}(\mathbf{k})$ given by Eq. (7) in the main text, and alternately stack the $H_{2D}^{(+)}(\mathbf{k})$ layer and the $H_{2D}^{(-)}(\mathbf{k})$ layer in the z direction. The Bloch Hamiltonian of the stacked layers is given by

$$H_{\mathcal{I}}(\mathbf{k}) = \begin{pmatrix} H_{2D}^{(+)}(\mathbf{k}) & H_{z,\mathcal{I}}(\mathbf{k}) \\ H_{z,\mathcal{I}}^{\dagger}(\mathbf{k}) & H_{2D}^{(-)}(\mathbf{k}) \end{pmatrix}, \quad (\text{S67})$$

where $H_{z,\mathcal{I}}(\mathbf{k})$ is the interlayer hopping expressed as

$$H_{z,\mathcal{I}}(\mathbf{k}) = \tau_x \otimes \begin{pmatrix} 0 & t_1 + t'_1 e^{-ik_z} \\ t_1 e^{-ik_z} + t'_1 & 0 \end{pmatrix} + i\tau_y \otimes \begin{pmatrix} t_2 + t'_2 e^{-ik_z} & 0 \\ 0 & -t_2 e^{-ik_z} - t'_2 \end{pmatrix}. \quad (\text{S68})$$

In this model, each layer respects inversion symmetry $\mathcal{I}H_{2D}^{(\pm)}(\mathbf{k})\mathcal{I}^{-1} = H_{2D}^{(\pm)}(-\mathbf{k})$ with $\mathcal{I} = \tau_z\sigma_y$. By choosing the inversion center at $z = 0$ in the unit cell, inversion symmetry for the overall Hamiltonian $H_{\mathcal{I}}(\mathbf{k})$ is written as

$$\mathcal{I}_{3D}H_{\mathcal{I}}(\mathbf{k})\mathcal{I}_{3D}^{-1} = H_{\mathcal{I}}(-\mathbf{k}), \quad \mathcal{I}_{3D} := \begin{pmatrix} 1 & 0 \\ 0 & e^{-ik_z} \end{pmatrix} \otimes \mathcal{I}, \quad (\text{S69})$$

where the matrix $\text{diag}(1, e^{-ik_z})$ acts on the sublattice degrees of freedom. Henceforth, we consider an odd number of layers to preserve inversion symmetry.

Here, we focus on the point-gap topology at $E = 0$ in the complex-energy spectrum [Fig. S5(a)]. Figure S5(b) shows that boundary states do not appear in the point gap around $E = 0$ under the OBC in the x direction and the PBC in the other directions (slab geometry). By contrast, Fig. S5(c) demonstrates that the boundary states with two exceptional points appear in the point gap around $E = 0$ under the OBC in the x and z directions and the PBC in the y direction. Due to inversion symmetry, these boundary states are localized at opposite hinges [Fig. S5(d)], each of which supports a single EP.

To characterize the exceptional second-order topological insulator protected by inversion symmetry, we introduce a Chern number in the slab geometry with the OBC in the z direction. Under weak interlayer coupling, the 3D model can be adiabatically connected to the 2D layers without couplings as long as the point gap is open. Thus, the Chern number in the slab geometry with such weak interlayer coupling is given by the sum of the Chern numbers ($\text{Ch}_1^{(l)}, \text{Ch}_2^{(l)}$) of each layer labeled by l ,

$$\text{Ch}_i^{\text{slab}} = \sum_l \text{Ch}_i^{(l)}, \quad (\text{S70})$$

with $i = 1, 2$, where l runs over all the layers. Since the number of layers is odd, the Chern numbers under the slab geometry are given by

$$(\text{Ch}_1^{\text{slab}}, \text{Ch}_2^{\text{slab}}) = (1, 0). \quad (\text{S71})$$

Therefore, our model can be regarded as a pseudo-2D exceptional topological insulator with a finite thickness in the z direction. Consequently, the hinge states with a single exceptional point appear under the OBC in the x direction.

The hinge state of the exceptional second-order topological insulator is protected against surface perturbations that preserve inversion symmetry in addition to chiral and sublattice symmetries. To see the importance of inversion symmetry, we consider an exceptional second-order topological insulator with an odd number of exceptional hinge channels. The even number of channels can be removed by moving them to the top and bottom hinges while preserving inversion symmetry (Fig. S6). On the other hand, the middle channel cannot be removed, and therefore this state is topologically protected by inversion symmetry. This scenario can also be applied to hinge states of the reflection-symmetric exceptional second-order topological insulators.

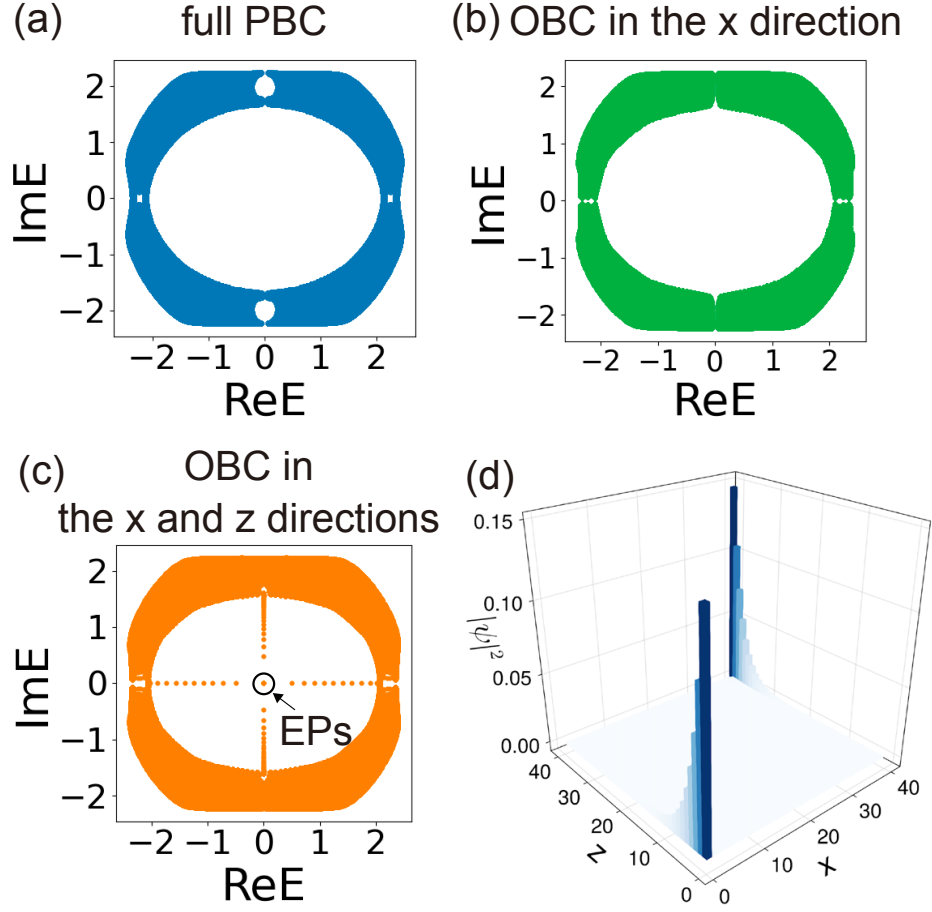


FIG. S5. Complex energy spectra of the exceptional second-order topological insulator protected by inversion symmetry under the (a) full periodic boundary conditions (PBC), (b) open boundary conditions (OBC) in the x direction and PBC in the y and z directions, and (c) OBC in the x and z directions and PBC in the y direction. “EPs” in (c) indicates exceptional points. (d) Real-space distribution of one of the right eigenstates encircled by the circle in (c). The parameters are $t_1 = 0.1$, $t'_1 = 0.2$, $t_2 = 0.3$, and $t'_2 = 0.25$. The system size in the x direction is 50 in (b). The system size is 40 in the x direction, and the number of layers is 79 in (c) and (d). The momentum resolutions in the k_i ($i = y, z$) direction are $\Delta k_i = 2\pi/80$ in the whole Brillouin zone in (b) and (c). For $-\pi/1000 \leq k_y \leq \pi/1000$, the momentum resolution is $\Delta k_y = 2\pi/40000$ to capture the energy spectra of the boundary states.

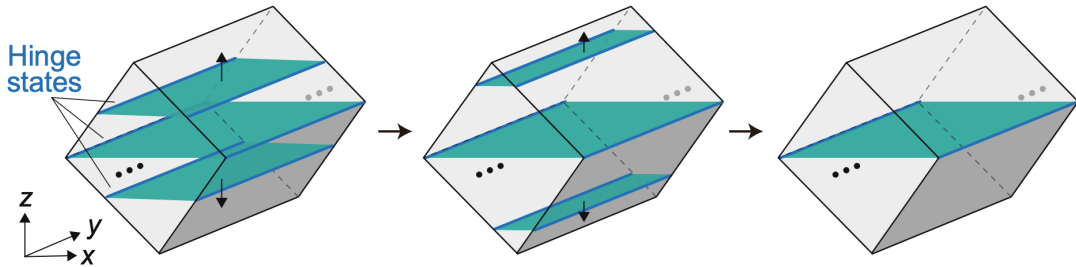


FIG. S6. Removing of an even number of hinge channels in an inversion-symmetric exceptional second-order topological insulator. The hinge channels except for the middle state can be removed by moving them to the top hinge and bottom hinge without breaking inversion symmetry.

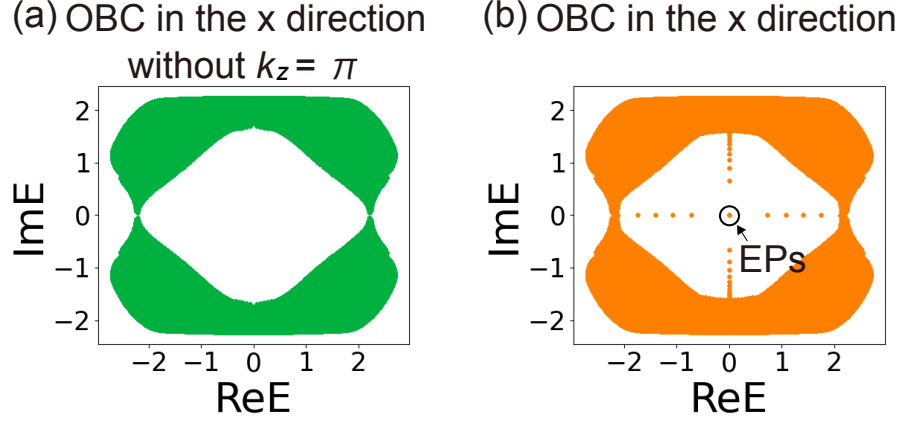


FIG. S7. Complex energy spectra of the Hamiltonian $H_{\mathcal{M}}(\mathbf{k})$ under the open boundary conditions (OBC) in the x direction and the periodic boundary conditions (PBC) in the y and z directions. (a) Energy spectrum at various k_z without $k_z = \pi$. (b) Energy spectrum in the whole k_x - k_y Brillouin zone including $k_z = \pi$. “EPs” in (b) indicates exceptional points. The parameters are the same as those in the main text. The system size is 50 in the x direction. The momentum resolutions in the k_i ($i = y, z$) direction are $\Delta k_i = 2\pi/80$. For $-\pi/100 < k_y < \pi/100$ and $k_z = \pi$, the momentum resolution is $\Delta k_y = 2\pi/20000$ to obtain the energy spectra of the surface states.

SV. 3D EXCEPTIONAL TOPOLOGICAL INSULATORS PROTECTED BY REFLECTION SYMMETRY

We discuss the surface states of the 3D reflection-symmetric exceptional second-order topological insulator $H_{\mathcal{M}}(\mathbf{k})$ given by Eq. (11) in the main text. In the main text, we have discussed the hinge states of $H_{\mathcal{M}}(\mathbf{k})$ under the OBC in the x and z directions with the surfaces perpendicular to the $(1, 0, 1)$ and $(1, 0, -1)$ directions. Here, we show that boundary states appear on the surfaces perpendicular to the x direction. A pair of the mirror Chern numbers for our model takes $(\text{Ch}_{\mathcal{M},1}, \text{Ch}_{\mathcal{M},2}) = (1, 0)$ at $k_z = \pi$.

We calculate the energy spectra of our model $H_{\mathcal{M}}(\mathbf{k})$. Figure S7(a) shows the energy spectrum without $k_z = \pi$ in the slab geometry with the OBC in the x direction with the y - z surface. This result without $k_z = \pi$ shows that surface states do not appear at $E = 0$ in the point gap. We also calculate the energy spectrum with the whole Brillouin zone including $k_z = \pi$ [Fig. S7(b)] and find that the surface states with four exceptional points appear in the point gap at $E = 0$.

Since our model has inversion symmetry, two of the four exceptional points are related to each other via inversion symmetry. Therefore, each y - z surface hosts two exceptional points. In addition, one of the two exceptional points belongs to the block $H_+(k_x, k_y, \pi)$, and the other belongs to $H_-(k_x, k_y, \pi)$. Therefore, these exceptional points in the different mirror blocks cannot be annihilated without breaking \mathcal{M} symmetry. The pair of the two exceptional points is characterized by the mirror Chern number $(\text{Ch}_{\mathcal{M},1}, \text{Ch}_{\mathcal{M},2}) = (1, 0)$ and hence topologically protected.